

SPECTRAL GROWTH IN $W(E_{10})$: DOUBLE COSET FILTRATION AND HILBERT GEOMETRY

KYOUNGHEE KIM

ABSTRACT. We study the spectral radii of elements in the hyperbolic Coxeter group $W(E_{10})$ by introducing a filtration indexed by reflections conjugate to a distinguished simple reflection s_0 . This filtration organizes $W(E_{10})$ into double cosets relative to the parabolic subgroup $W(A_9)$, and we classify the minimal representatives of these cosets via a rooted directed acyclic graph (DAG) labeled by triples. Each node in the DAG corresponds to a structured reflection composition, enabling a recursive understanding of spectral growth. Using the Hilbert metric on the Tits cone, we relate spectral radii to geometric displacement and demonstrate an effective method to compute the spectral radii inductively. This provides a geometric and combinatorial framework for understanding the Weyl spectrum of $W(E_{10})$. While our focus is on E_{10} , the techniques developed extended naturally to the family $W(E_n)$ for $n \geq 10$, with implications for dynamics on rational surfaces and entropy spectra of surface automorphisms.

1. INTRODUCTION

Hyperbolic Coxeter groups form a cornerstone of modern geometric group theory, with deep connections to hyperbolic geometry, Kac-Moody algebras, and arithmetic reflection groups. Since the foundational work of Vinberg [26] on hyperbolic reflection groups, these groups have served as central examples in the study of discrete symmetries and tessellations of non-Euclidean spaces. Among them, the Coxeter group $W(E_{10})$ stands out as the unique simply-laced hyperbolic Coxeter group of rank 10. It plays a prominent role in both geometric and arithmetic settings, and appears naturally in the spectral dynamics of automorphisms of rational surfaces of Picard rank 11 [20, 21, 1, 9, 17].

This article introduces a new framework for organizing and analyzing the spectral behavior of elements in $W(E_{10})$, based on a filtration indexed by the distinguished simple reflection s_0 at the branching node of the E_{10} Dynkin diagram. Our approach centers on the structure of conjugates of s_0 , placing it in close proximity to the theory of reflection length. The reflection length in infinite and hyperbolic Coxeter groups has received substantial attention in recent years; see, for example, [19, 11, 10, 18].

We define the s_0 -level of an element $\omega \in W(E_{10})$, denoted $h_{s_0}(\omega)$, as the minimal number of occurrences of s_0 in any reduced word among all conjugates of ω . This statistic induces a natural *filtration by double cosets*:

$$\mathcal{D}_{n,n} := \{\omega \in W(E_{10}) : \omega \in W(A_9)\kappa W(A_9) \text{ with } h_{s_0}(\omega) = n\},$$

where κ is the unique Bruhat-minimal representative of its double coset.

In Section 3 and Section 4, we give a combinatorial classification of these minimal representatives using ordered triples from the set

$$T = \{i, j, k \subset \{1, \dots, 10\} : 1 \leq i < j < k \leq 10\}.$$

2020 *Mathematics Subject Classification.* 20F55, 51F15, 20E45, 14J50, 14E07.

Key words and phrases. Hyperbolic Coxeter group $W(E_{10})$, Spectral radius, Hilbert metric, Tits cone, Salem numbers, Reflection length, Bruhat Order.

For each s_0 -level n , the corresponding minimal representatives are encoded by an inductively defined finite set $T_n \subset T^n$ of ordered n -tuples of triples. This leads to a natural identification of minimal double coset representatives with nodes in a *rooted directed acyclic graph* (DAG), where each node is labeled by a triple in T , and directed edges represent the addition of a new triple during the recursive construction.

Theorem (Triple-Labeled Graph Structure of Minimal Representatives, Theorem 4.3). *Let $\mathcal{D}_{n,n}$ denote the set of elements in $W(E_{10})$ of s_0 -level n (as defined in (4.1)), and let $K \subset W(E_{10})$ be the set of Bruhat-minimal representatives of double cosets $W(A_9) \backslash W(E_{10}) / W(A_9)$.*

Then:

- (1) *Each $\kappa \in K \cap \mathcal{D}_{n,n}$ is uniquely determined by an ordered n -tuple of triples from*

$$T := \{\{i, j, k\} \subset \{1, \dots, 10\} : 1 \leq i < j < k \leq 10\}.$$

- (2) *There exists a rooted directed acyclic graph (DAG) \mathcal{G} , whose depth- n nodes correspond bijectively to a finite inductively defined subset $T_n \subset T^n$, such that each directed path of length n encodes the recursive construction of a minimal double coset representative $\kappa \in \mathcal{D}_{n,n}$.*

This DAG encodes the combinatorial growth of minimal representatives and provides a canonical framework for tracking how new reflections from s_0 -conjugacy classes are introduced. Each directed path in the graph corresponds to a specific representative $\kappa \in W(E_{10})$ with s_0 -level n , and thus serves as a backbone for understanding the spectral stratification of $W(E_{10})$.

Associated to each level n , we define a finite *spectral set*:

$$\Lambda_n := \{\rho(\omega) : \omega \in \mathcal{D}_{n,n}\},$$

consisting of the spectral radii of elements constructed from n reflections in s_0 -conjugacy classes. This construction yields a new filtration of the spectral data of $W(E_{10})$, revealing levelwise structure and exponential growth.

Theorem (Spectral Monotonicity, Theorem 5.7). *Let $\{\Lambda_k(\widehat{I}^{(k)})\}_{k \geq 1}$ be the sequence of spectral subsets associated with a directed path in the s_0 -growth graph. Then the sequences of minima and maxima are non-decreasing in s_0 -level k :*

$$\min \Lambda_k(\widehat{I}^{(k)}) \leq \min \Lambda_{k+1}(\widehat{I}^{(k+1)}), \quad \max \Lambda_k(\widehat{I}^{(k)}) \leq \max \Lambda_{k+1}(\widehat{I}^{(k+1)}) \quad \text{for all } k \geq 1.$$

Theorem (Spectral Exhaustion Theorem, Theorem 5.8). *For every $C > 1$, there exists an integer $N \geq 1$ such that*

$$\{\rho(\omega) \in \mathbb{R} : \omega \in W(E_{10}), \rho(\omega) \leq C\} \subset \bigcup_{n \leq N} \Lambda_n.$$

We further interpret this filtration geometrically using the Hilbert metric on the Tits cone of $W(E_{10})$, and prove that the spectral envelopes Λ_n grow monotonically in n . This leads to a levelwise recursive method for computing all spectral radii in $W(E_{10})$ below a given threshold, with special attention to the emergence and density of primitive Salem numbers.

Theorem (Hilbert Ball Inclusion of Level- n Elements, Theorem 5.11). *Let x be a point in the interior of the fundamental chamber. Define $B_n := B_K(x, t_n) \subset \mathcal{C}$ to denote the Hilbert ball of radius.*

$$t_n := \inf \{\delta(\omega) : \omega \in \mathcal{D}_{n,n}\}.$$

Then for any $\omega \in W(E_{10})$, if $\omega \cdot x \in B_n$, the s_0 -level of ω satisfies $h_{s_0}(\omega) \leq n$.

Our computations reveal the set of Salem numbers that are contained in Λ_n . We isolated the primitive part $\hat{\Lambda}_n \subset \Lambda_n$ —the set of Salem numbers whose k^{th} root is not a Salem number for $k \geq 2$ —which emerges at level n , and observe experimentally that their number grows approximately fivefold at each step:

$$|\hat{\Lambda}_n| \approx 5 \cdot |\hat{\Lambda}_{n-1}|, \quad \text{for } n \geq 2.$$

This spectral growth has a precise geometric manifestation. Via McMullen’s theory of Hilbert metrics on the Tits cone \mathcal{C} , we prove that the level sets $\mathcal{D}_{n,n}$ are confined outside a sequence of *nested Hilbert balls* with a fixed base point x in the fundamental domain

$$B_n := B_K(x, t_n), \quad t_n \sim \log m_n,$$

where $m_n := \min \Lambda_n$. Thus, the s_0 –filtration yields a geometric stratification of the Tits cone that reflects the spectral radius of elements and the depth of their reflection complexity.

The computations and structures developed in this work support the emergence of a rich and previously uncharted spectral hierarchy inside the Coxeter group $W(E_{10})$. Guided by the recursive growth of minimal double coset representatives and their interaction with the Hilbert metric on the Tits cone, our data suggest the following:

Conjecture (Spectral Growth Conjecture). *Let $\Lambda_n \subset \mathbb{R}_{>1}$ denote the set of spectral radii of $W(E_{10})$ -elements arising at s_0 –level n . Then:*

- (i) *The maximal values satisfy the exact relation*

$$M_n = M_1^n, \quad n \geq 1,$$

as proved in Lemma 5.9. Moreover, the minimal extreme values appear to obey an approximate geometric scaling:

$$m_n \approx \delta^{n-2} M_{n-1}, \quad \text{for } n \geq 3,$$

for some $0 < \delta < 1$. Here “ \approx ” indicates numerical proximity.

- (ii) *The number of new primitive Salem numbers at level n , denoted $|\hat{\Lambda}_n|$, grows exponentially with n :*

$$|\hat{\Lambda}_n| \sim C \cdot r^n, \quad \text{with } r \approx 5.$$

- (iii) *The maximal spectral gap between consecutive elements in $\hat{\Lambda}_n$ decays exponentially, and the primitive spectrum becomes increasingly dense as $n \rightarrow \infty$.*

These observations suggest that the s_0 –growth graph encodes not just the combinatorial unfolding of $W(E_{10})$, but also a kind of spectral stratification geometry: new eigenvalues emerge along specific paths, bounded within nested Hilbert balls, and propagate upward in a controlled yet rapidly diversifying manner. We anticipate that this framework will offer new insights into both the representation theory and geometric group theory of hyperbolic Coxeter groups.

Remark 1.1. *Kim [16] investigated the closure (the Weyl spectrum) of the set of spectral radii in $\bigcup_n W(E_n)$, establishing monotonicity with respect to the Coxeter rank n . In contrast, the present article fixes the Coxeter rank $n = 10$ and studies spectral growth via the s_0 –level filtration—the minimal number of occurrences of the distinguished reflection s_0 in the conjugacy class.*

Connection to Entropy Spectrum of Rational Surface Automorphisms Suppose X is a rational surface. By Nagata [22, 23], an automorphism $f : X \rightarrow X$ is a lift of a birational map on $\mathbf{P}^2(\mathbb{C})$. Also, by the identification between the intersection product and a symmetric Bilinear form on a Minkowski space, if f has an infinite order, then the induced action f_* on the Picard group of X is an element of the Coxeter group $W(E_n)$ where $n+1$ is the Picard rank of X . The topological entropy of f is determined by the spectral radius of f_* as an action on a real vector space:

$$h_{\text{top}}(f) = \log \rho(f_*|_{\text{Pic}(X)}).$$

It is known that the logarithm of every spectral radius of $\bigcup_n W(E_n)$ arises as the topological entropy of a rational surface automorphism [7, 21, 25, 17]. Moreover, the closure of this set—often called the *Weyl spectrum*—coincides with the closure of the set of exponentials of topological entropies of rational surface automorphisms [8, 4]. However, since many elements $\omega \in \bigcup_n W(E_n)$ can share the same spectral radius, identifying which element corresponds to a geometric realization is often nontrivial.

Recent results by Uehara [25] and Kim [17, Theorem B] show that for each $\omega \in W(E_n)$, there exists a representative $\omega' \in W(E_n)$ obtained by multiplying ω with elements of the parabolic subgroup $W(A_n) \subset W(E_n)$, such that $\rho(\omega') = \rho(\omega)$ and ω' is realized as the induced action on the Picard group of a rational surface automorphism $f : X \rightarrow X$. In particular, one obtains the identity

$$S_{10} := \{h_{top}(f) : f \in \text{Aut}(X), \text{ rank of } \text{Pic}(X) = 11\} = \log\{\rho(\omega) : \omega \in W(E_{10})\}.$$

Our results provide a complete, recursive framework for computing this spectrum. In particular, we determine (recursively) the full set of topological entropies arising from automorphisms of rational surfaces with Picard rank 11. It is noteworthy that, based on Table 1 and Table 2, all elements of $S_{10} \cap (0, 0.36)$ appear to arise from quadratic rational surface automorphisms.

Organization. This article is organized as follows. In Section 2, we provide a brief review of Coxeter groups and related background relevant to the remainder of the paper. Section 3 introduces the notion of s_0 -length and constructs the Bruhat-minimal representatives for double cosets with respect to the parabolic subgroup $W(A_9)$. In Section 4, we define the s_0 -level and describe the associated rooted directed acyclic graph (DAG) that encodes the recursive structure of minimal representatives. Section 5 presents the main theorems and geometric interpretation using the Hilbert metric, along with supporting numerical results. Appendix A contains a complete list of primitive Salem numbers and their minimal polynomials in $\hat{\Lambda}_2$, and the first 50 such numbers in $\hat{\Lambda}_3$. Finally, Appendix B includes a ready-to-use SageMath script for generating the ordered triples associated with Bruhat-minimal representatives.

2. COXETER GROUP $W(E_{10})$

In this section, we briefly summarize the structure and properties of the Coxeter group $W(E_{10})$. While many of these features hold for general Coxeter groups, we focus on those most relevant to our context. For background and comprehensive treatment, see [3, 14].

The group $W(E_{10})$ is the simply-laced hyperbolic Coxeter group of type E_{10} —a rank-10 indefinite extension of the finite type E_8 . It is generated by ten involutions $\{s_i : i = 0, 1, \dots, 9\}$, one for each node of the Dynkin diagram in Figure 1, subject to the standard Coxeter relations:

$$(s_i s_j)^{m_{ij}} = 1,$$

where $m_{ii} = 1$, $m_{ij} = 3$ if nodes are joined by an edge, and $m_{ij} = 2$ otherwise.

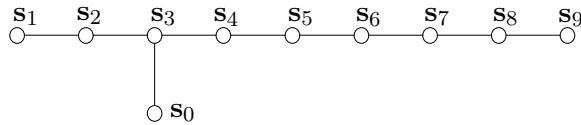


FIGURE 1. Dynkin diagram of E_{10}

Every element $\omega \in W(E_{10})$ can be written as a product of generators:

$$\omega = g_1 g_2 \cdots g_k, \quad g_i \in S.$$

The *length* $\ell(\omega)$ is the minimal such k , and the corresponding expression is called a *reduced word* or *reduced expression*. Elements of $W(E_{10})$ generally admit multiple reduced words.

A foundational result in Coxeter theory, due to Tits and Matsumoto, ensures that all reduced expressions for the same element are connected by a sequence of Coxeter (braid) relations.

Theorem 2.1 (Matsumoto's Theorem [3, Theorem 3.3.1]). *Let (W, S) be a Coxeter system and let $\omega \in W$.*

- (1) *Any expression $g_1 g_2 \cdots g_q$ with $g_i \in S$ representing ω can be transformed into a reduced expression by a sequence of nil-moves (deleting adjacent squares $s_i^2 = 1$) and Coxeter (braid) relations.*
- (2) *Any two reduced expressions for ω are connected by a sequence of Coxeter relations.*

Let $\mathbb{R}^{1,10}$ be a real vector space with orthonormal basis $(\mathbf{e}_0, \mathbf{e}_1, \dots, \mathbf{e}_{10})$, where

$$\mathbf{e}_0^2 = 1, \quad \mathbf{e}_i^2 = -1 \text{ for } i \geq 1, \quad \mathbf{e}_i \cdot \mathbf{e}_j = 0 \text{ for } i \neq j.$$

This defines a symmetric bilinear form of signature $(1, 10)$ on $\mathbb{R}^{1,10}$.

Let $V \subset \mathbb{R}^{1,10}$ be the subspace spanned by the ten simple roots $\{\alpha_0, \dots, \alpha_9\}$, where

$$\alpha_0 = \mathbf{e}_0 - \mathbf{e}_1 - \mathbf{e}_2 - \mathbf{e}_3, \quad \alpha_i = \mathbf{e}_i - \mathbf{e}_{i+1} \text{ for } i = 1, \dots, 9.$$

This root system defines the E_{10} Dynkin diagram. The inner products among the roots satisfy

$$B(\alpha_i, \alpha_j) := -\alpha_i \cdot \alpha_j = \begin{cases} 2 & \text{if } i = j, \\ -1 & \text{if } i \neq j \text{ and } i \sim j, \\ 0 & \text{otherwise,} \end{cases}$$

where $i \sim j$ denotes adjacency in the diagram. Equivalently,

$$B(\alpha_i, \alpha_j) = -2 \cos\left(\frac{\pi}{m_{ij}}\right).$$

Each root α_i defines a reflection $\mathbf{s}_i : V \rightarrow V$ given by

$$\mathbf{s}_i(v) := v - B(v, \alpha_i) \alpha_i = v + (v \cdot \alpha_i) \alpha_i.$$

This is the standard reflection across the hyperplane orthogonal to α_i , satisfying $\mathbf{s}_i(\alpha_i) = -\alpha_i$ and fixing the orthogonal complement.

Define a linear representation

$$\sigma : W(E_{10}) \rightarrow \mathrm{GL}(V), \quad \sigma(s_i) := \mathbf{s}_i.$$

This representation is a faithful representation of $W(E_{10})$ that preserve the bilinear form B ; see [14, Cor. 5.4]. The action of $W(E_{10})$ on the Lorentzian space V gives rise to the Tits cone, a fundamental geometric domain we will discuss via Hilbert metrics in Section 5.

Spectral Radius. For each $\omega \in W(E_{10})$, the linear operator $\sigma(\omega)$ acts on V by a Lorentzian isometry with matrix representation M_ω in the basis $\{\mathbf{e}_0, \mathbf{e}_1, \dots, \mathbf{e}_{10}\}$. We define the *spectral radius* of ω by

$$\rho(\omega) := \rho(M_\omega),$$

where $\rho(M)$ denotes the spectral radius (largest modulus of eigenvalues) of the matrix M .

2.1. **Bruhat Order.** Let (W, S) be a Coxeter system, and let

$$R = \{ \omega s \omega^{-1} : \omega \in W, s \in S \}$$

denote the set of reflections in W . For $\omega', \omega \in W$, we write

$$\omega' \rightarrow \omega \quad \text{if} \quad \omega = \omega' r \quad \text{for some } r \in R, \quad \text{and} \quad \ell(\omega) > \ell(\omega').$$

The (*strong*) *Bruhat order* on W is the partial order defined by:

$$\omega' \leq_{\text{Bruhat}} \omega \iff \text{there exists a chain } \omega' = \omega_0 \rightarrow \omega_1 \rightarrow \cdots \rightarrow \omega_k = \omega.$$

Equivalently, $\omega' \leq_{\text{Bruhat}} \omega$ if every reduced expression for ω contains a subword that is a reduced expression for ω' .

This partial order turns $(W, \leq_{\text{Bruhat}})$ into a directed poset known as the *Bruhat poset*, with unique minimal element the identity 1.

Bruhat order is graded by the length function and is compatible with multiplication:

$$\omega' <_{\text{Bruhat}} \omega \Rightarrow \ell(\omega') < \ell(\omega),$$

and for any $s \in S$,

$$\omega' \leq_{\text{Bruhat}} \omega \text{ and } \ell(\omega') = \ell(\omega) - 1 \Rightarrow \omega' s \leq_{\text{Bruhat}} \omega s.$$

We record a useful technical lemma that arises in spectral and length considerations:

Lemma 2.2 ([3, Lemma 2.2.10]). *Suppose $x <_{\text{Bruhat}} xr$ and $y <_{\text{Bruhat}} ry$ for $x, y \in W$ and $r \in R$. Then*

$$xy <_{\text{Bruhat}} xry.$$

Unique Bruhat-minimal Representative For $J \subset S$, the subgroup $W_J \subset W$ generated by the set J is called a *parabolic subgroup*. Define the set of minimal left coset representatives by

$$W^J := \{ \omega \in W : \ell(\omega s) > \ell(\omega) \text{ for all } s \in J \}.$$

Then every $\omega \in W$ admits a unique factorization

$$\omega = uv, \quad \text{with } u \in W^J, v \in W_J,$$

satisfying the length additivity

$$\ell(\omega) = \ell(u) + \ell(v).$$

Moreover, each double coset $W_J \omega W_J$ contains a unique representative of minimal length with respect to the Bruhat order (see Deodhar [6]).

3. $W(A_9)$ -DOUBLE COSETS

The finite Coxeter group $W(A_9)$ embeds naturally as a (parabolic) subgroup of the hyperbolic Weyl group $W(E_{10})$ by restricting to an appropriate subset of simple reflections. We regard

$$W(A_9) \cong \langle s_1, s_2, \dots, s_9 \rangle < W(E_{10}),$$

as the stabilizer of the isotropic vector \mathbf{e}_0 in the standard basis $\{\mathbf{e}_0, \mathbf{e}_1, \dots, \mathbf{e}_{10}\}$ of the Lorentzian lattice, where

$$\mathbf{e}_0^2 = 1, \quad \mathbf{e}_i^2 = -1 \quad (i \geq 1), \quad \mathbf{e}_i \cdot \mathbf{e}_j = 0 \quad (i \neq j).$$

Let

$$T = \{ \{i, j, k\} \subset \{1, \dots, 10\} \mid 1 \leq i < j < k \leq 10 \}$$

be the set of 3-subsets of $\{1, \dots, 10\}$. For $I = \{i, j, k\} \in T$, let κ_I denote the reflection in the root $\mathbf{e}_0 - \mathbf{e}_i - \mathbf{e}_j - \mathbf{e}_k$.

Equivalently, if $\sigma \in W(A_9) \cong S_{10}$ is any element with $\sigma(\{1, 2, 3\}) = \{i, j, k\}$, then

$$\kappa_{\{i, j, k\}} = \sigma s_0 \sigma^{-1}.$$

In particular, every $\kappa_{\{i,j,k\}}$ is $W(A_9)$ -conjugate to $s_0 = \kappa_{\{1,2,3\}}$.

Lemma 3.1. *For each element $\omega \in W(E_{10}) \setminus W(A_9)$, there exist a positive integer $n > 0$ and triples $I_1, I_2, \dots, I_n \in T$ such that*

$$\omega = \rho_L \kappa_{I_1} \kappa_{I_2} \cdots \kappa_{I_n} \rho_R,$$

where $\rho_L, \rho_R \in W(A_9)$.

Proof. Since $W(E_{10})$ is generated by $W(A_9)$ together with s_0 , every element $\omega \in W(E_{10}) \setminus W(A_9)$ can be written as

$$\omega = \rho_{k+1} s_0 \rho_k s_0 \cdots s_0 \rho_1 s_0 \rho_0, \quad \rho_i \in W(A_9),$$

where $k \geq 0$ denotes the number of occurrences of s_0 in the reduced word.

—
If $k = 0$, then

$$\omega = \rho_1 s_0 \rho_0 = \rho_1 \kappa_{\{1,2,3\}} \rho_0,$$

which already has the desired form.

For $k = 1$, we have

$$\omega = \rho_2 \rho_1 (\rho_1^{-1} s_0 \rho_1) s_0 \rho_0.$$

Let $I = \{i_1, i_2, i_3\} := \rho_1^{-1}(\{1, 2, 3\})$. Then $\rho_1^{-1} s_0 \rho_1$ is the reflection through $\alpha_I = e_0 - e_{i_1} - e_{i_2} - e_{i_3}$, hence $\rho_1^{-1} s_0 \rho_1 = \kappa_I$. Therefore

$$\omega = (\rho_2 \rho_1) \kappa_I s_0 \rho_0.$$

—
The general case follows by induction on k . Define $\eta_j = \rho_j \rho_{j-1} \cdots \rho_1$ for $1 \leq j \leq k+1$, and set $I_j = \eta_j^{-1}(\{1, 2, 3\})$. Then

$$\eta_j^{-1} s_0 \eta_j = \kappa_{I_j},$$

and substituting successively yields

$$\omega = \eta_{k+1} (\eta_k^{-1} s_0 \eta_k) \cdots (\eta_1^{-1} s_0 \eta_1) s_0 \rho_0 = \eta_{k+1} \kappa_{I_k} \cdots \kappa_{I_1} s_0 \rho_0.$$

Setting $\rho_L = \eta_{k+1}$ and $\rho_R = \rho_0$ gives the desired decomposition. \square

Geometric interpretation. The decomposition in Lemma 3.1 shows that each double coset

$$W(A_9) \omega W(A_9) \subset W(E_{10}) \setminus W(A_9)$$

admits a representative of the form $\kappa_{I_1} \kappa_{I_2} \cdots \kappa_{I_n}$, where each κ_{I_j} is a reflection through the hyperplane orthogonal to $\alpha_{I_j} = e_0 - e_{i_1} - e_{i_2} - e_{i_3}$, a $W(A_9)$ -conjugate of the simple root α_0 . Geometrically, these double cosets parametrize the relative positions of $W(A_9)$ -chambers in the Tits cone: composing successive κ_{I_j} corresponds to crossing hyperplanes parallel (under the $W(A_9)$ -action) to the distinguished face H_0 of the fundamental chamber. Thus, each step in the product moves a base point deeper into the cone, increasing its s_0 -level (defined in Section 3), and the $W(A_9)$ -double cosets provide a natural stratification of $W(E_{10})$ according to this relative height.

s_0 -length. For any element $\omega \in W(E_{10})$, define

$$|\omega|_{s_0} := \min \left\{ \text{number of occurrences of } s_0 \text{ in a reduced expression of } \omega \right\}.$$

We call $|\omega|_{s_0}$ the s_0 -length of ω . Because braid relations (e.g. $s_0 s_3 s_0 = s_3 s_0 s_3$) may change the raw count of s_0 in a reduced word, we take the minimum over all reduced expressions (Matsumoto's theorem ensures that all reduced words are connected by braid moves).

Since each κ_I ($I \in T$) is a $W(A_9)$ -conjugate of s_0 , every κ_I contains exactly one s_0 in any reduced expression. Consequently, if $|\omega|_{s_0} = n$, then there exist triples $I_1, \dots, I_n \in T$ such that

$$\omega \in W(A_9) \kappa_{I_1} \kappa_{I_2} \cdots \kappa_{I_n} W(A_9),$$

but

$$\omega \notin W(A_9) \kappa_{I_1} \kappa_{I_2} \cdots \kappa_{I_j} W(A_9) \quad \text{for any } j < n.$$

3.1. Representatives of Double Cosets. To investigate the algebraic structure of the double-coset space

$$W(A_9) \backslash W(E_{10}) / W(A_9),$$

we begin by examining the relations among the reflections κ_I for $I \in T$.

Lemma 3.2. *Let $I, J \in T$. Then the products of the corresponding reflections κ_I and κ_J satisfy the following relations:*

- (1) *If $|I \cap J| = 3$, then $\kappa_I \kappa_J = \text{id}$.*
- (2) *If $|I \cap J| = 2$, then $\kappa_I \kappa_J = \kappa_I \rho = \rho \kappa_J$, where $\rho \in W(A_9)$ is the reflection through the root $\mathbf{e}_i - \mathbf{e}_j$, with i, j being the two indices not shared by I and J .*
- (3) *If $|I \cap J| = 1$, then $\kappa_I \kappa_J = \kappa_J \kappa_I$ and $|\kappa_I \kappa_J|_{s_0} = 2$.*
- (4) *If $|I \cap J| = 0$, then $\kappa_I \kappa_J \kappa_I = \kappa_J \kappa_I \kappa_J$ and $|\kappa_I \kappa_J|_{s_0} = 2$.*

These relations mirror the local Coxeter structure determined by the intersection pattern of the index sets I and J . In particular, the cases $|I \cap J| = 2, 1, 0$ correspond respectively to types A_2 , $A_1 \times A_1$, and A_2 within the subdiagram of the Coxeter graph generated by κ_I and κ_J .

Proof. After relabelling indices if necessary, we may assume $I = \{1, 2, 3\}$. By considering

$$J = \{1, 2, 3\}, \quad \{1, 2, 4\}, \quad \{1, 4, 5\}, \quad \text{and} \quad \{4, 5, 6\},$$

one obtains representatives for the cases $|I \cap J| = 3, 2, 1, 0$, respectively. A direct computation using the defining action of κ_I on the basis vectors $\mathbf{e}_0, \mathbf{e}_1, \dots, \mathbf{e}_{10}$ confirms the stated relations in each case. \square

Corollary 3.3. *Let $\omega \in W(E_{10})$. Then:*

- (1) *If $|\omega|_{s_0} = 1$, then $\omega \in W(A_9) \kappa_{\{1,2,3\}} W(A_9)$.*
- (2) *If $|\omega|_{s_0} = 2$, then either*

$$\omega \in W(A_9) \kappa_{\{1,4,5\}} \kappa_{\{1,2,3\}} W(A_9) \quad \text{or} \quad \omega \in W(A_9) \kappa_{\{4,5,6\}} \kappa_{\{1,2,3\}} W(A_9).$$

Proof. As noted earlier, for each $I \in T$, κ_I is $W(A_9)$ -conjugate to s_0 . If $|\omega|_{s_0} = 2$, then after relabelling the indices (via a permutation in S_{10}), the conclusion follows immediately from Lemma 3.2. \square

Another interesting relation arises when we consider three κ 's.

Lemma 3.4. *Let $I, J, K \in T$ satisfy*

$$|I \cap J| = |J \cap K| = |K \cap I| = 1.$$

Then the products of the corresponding reflections κ_I , κ_J , and κ_K satisfy:

- (1) *If $|I \cap J \cap K| = 1$, then $|\kappa_I \kappa_J \kappa_K|_{s_0} = 3$.*
- (2) *If $|I \cap J \cap K| = 0$, then $|\kappa_I \kappa_J \kappa_K|_{s_0} = 2$.*

Proof. Suppose first that $|I \cap J \cap K| = 1$. Without loss of generality, we may take

$$I = \{1, 6, 7\}, \quad J = \{1, 4, 5\}, \quad K = \{1, 2, 3\}.$$

A direct computation using the action of κ_I on the basis vectors $\mathbf{e}_0, \mathbf{e}_1, \dots, \mathbf{e}_{10}$ shows that

$$\begin{aligned} \kappa_I \kappa_J \kappa_K : \mathbf{e}_0 &\mapsto 4\mathbf{e}_0 - 3\mathbf{e}_1 - \mathbf{e}_2 - \mathbf{e}_3 - \mathbf{e}_4 - \mathbf{e}_5 - \mathbf{e}_6 - \mathbf{e}_7, \\ \mathbf{e}_1 &\mapsto 3\mathbf{e}_0 - 2\mathbf{e}_1 - \mathbf{e}_2 - \mathbf{e}_3 - \mathbf{e}_4 - \mathbf{e}_5 - \mathbf{e}_6 - \mathbf{e}_7. \end{aligned}$$

Since any element of $W(A_9)$ acts as a permutation of the vectors e_1, \dots, e_{10} , we see that

$$\kappa_I \kappa_J \kappa_K \notin W(A_9) \{\text{id}, \kappa_{\{1,2,3\}}, \kappa_{\{1,4,5\}} \kappa_{\{1,2,3\}}, \kappa_{\{4,5,6\}} \kappa_{\{1,2,3\}}\} W(A_9).$$

By Corollary 3.3, it follows that $|\kappa_I \kappa_J \kappa_K|_{s_0} = 3$.

If $|I \cap J \cap K| = 0$, we may take

$$I = \{2, 4, 6\}, \quad J = \{1, 4, 5\}, \quad K = \{1, 2, 3\}.$$

A direct computation shows that

$$\kappa_I \kappa_J \kappa_K = \rho_1 \rho_2 \kappa_{\{4, 5, 6\}} \kappa_{\{1, 2, 3\}} \rho_3,$$

where ρ_1 , ρ_2 , and ρ_3 are reflections through $\mathbf{e}_1 - \mathbf{e}_6$, $\mathbf{e}_2 - \mathbf{e}_5$, and $\mathbf{e}_3 - \mathbf{e}_4$, respectively. Hence $|\kappa_I \kappa_J \kappa_K|_{s_0} = 2$. \square

Notation. To simplify notation, for $I_1, \dots, I_n \in T$ we write

$$\kappa_{I_1, \dots, I_n} := \kappa_{I_1} \kappa_{I_2} \cdots \kappa_{I_n},$$

the product of the corresponding reflections in $W(E_{10})$.

Proposition 3.5. *For each integer $n \geq 0$, there exists a finite set T_n of ordered n -tuples in T with the following property: for every element $\omega \in W(E_{10})$ satisfying $|\omega|_{s_0} = n$, there exists a unique*

$$(I_1, I_2, \dots, I_n) \in T_n$$

such that

$$\omega \in W(A_9) \kappa_{I_1, \dots, I_n} W(A_9).$$

In particular, the double cosets

$$\{ W(A_9) \kappa_{I_1, \dots, I_n} W(A_9) : (I_1, \dots, I_n) \in T_n \}$$

form a complete set of representatives for the elements of $W(E_{10})$ at s_0 -length n .

Proof. Since T is finite, there are only finitely many ordered n -tuples $(I_1, \dots, I_n) \in T^n$, and hence finitely many double cosets of the form $W(A_9) \kappa_{I_1, \dots, I_n} W(A_9)$. Choosing one representative n -tuple from each distinct double coset yields a finite set T_n satisfying the desired property. \square

Definition 3.6 (Transformation data). *For each ordered n -tuple $\hat{I} = (I_1, \dots, I_n) \in T^n$, consider the corresponding product of reflections*

$$\kappa_{\hat{I}} := \kappa_{I_1} \kappa_{I_2} \cdots \kappa_{I_n}.$$

The action of $\kappa_{\hat{I}}$ on the basis $\{e_0, e_1, \dots, e_{10}\}$ is represented by a matrix M . We call this matrix representation the transformation data of \hat{I} , and denote it by

$$\text{Trans}(\hat{I}) := M.$$

Since $\hat{I} \in T^n$, the product $\kappa_{\hat{I}}$ has s_0 -length n , that is,

$$|\kappa_{\hat{I}}|_{s_0} = n.$$

We say that \hat{I} has s_0 -length n if $|\kappa_{\hat{I}}|_{s_0} = n$.

3.1.1. *Representing Triples.* For $n = 1$ and $n = 2$, the sets T_1 and T_2 consist of one and two elements, respectively, corresponding to the double cosets described in Corollary 3.3. The relations among triples of reflections established in Lemma 3.4 govern the structure of T_3 and the higher-level sets T_n . To construct T_n explicitly and understand how successive triples interact, we first analyze the adjacency relations among the triples in an ordered tuple. This analysis provides the combinatorial data from which T_n will later be defined recursively.

According to Lemma 3.2, maintaining the s_0 -length imposes restrictions on the intersections of consecutive triples in T_n .

Lemma 3.7 (Adjacency constraint). *Let $\widehat{I} = (I_1, \dots, I_n) \in T^n$. Then for each k ,*

$$|I_k \cap I_{k+1}| \in \{0, 1\}, \quad 1 \leq k \leq n-1.$$

Proof. Since $\widehat{I} = (I_1, \dots, I_n) \in T^n$, the corresponding product of reflections $\kappa_{\widehat{I}} = \kappa_{I_1} \cdots \kappa_{I_n}$ has s_0 -length equal to n . The claim follows directly from Lemma 3.2. \square

3.1.2. *Recursive construction of T_n from T_2 .* We start from

$$T_2 = \{ I^{(1)} = (\{1, 4, 5\}, \{1, 2, 3\}), I^{(2)} = (\{4, 5, 6\}, \{1, 2, 3\}) \},$$

as provided by Corollary 3.3. For T_3 , any ordered triple $\widehat{I} = (I_1, I_2, I_3)$ of s_0 -length 3 must arise (up to the $W(A_9)$ -double coset relation) by adjoining a single triple $I \in T$ to one of these pairs. Without loss of generality we place the new triple first and write

$$\widehat{I} = (I, I_1^{(j)}, I_2^{(j)}), \quad j \in \{1, 2\}.$$

Adjacency filter. By Lemma 3.7, minimality of the s_0 -length forces $|I \cap I_1^{(j)}| \in \{0, 1\}$. We first enumerate the finite set

$$\mathcal{C}_j = \{ I \in T : |I \cap I_1^{(j)}| \in \{0, 1\} \}.$$

(Practically, we retain those I with $|I \cap I_1^{(j)}| = 1$ as the primary branch and treat the 0-adjacency branch only when it survives the next test.)

Level test via the three- κ lemma: For each $I \in \mathcal{C}_j$, apply Lemma 3.4 to the triple $(I, I_1^{(j)}, I_2^{(j)})$. If all pairwise intersections are 1, then

$$|I \cap I_1^{(j)}| = |I_1^{(j)} \cap I_2^{(j)}| = |I_2^{(j)} \cap I| = 1,$$

and Lemma 3.4 distinguishes two outcomes:

$$|I \cap I_1^{(j)} \cap I_2^{(j)}| = \begin{cases} 1 & \Rightarrow |\kappa_I \kappa_{I_1^{(j)}} \kappa_{I_2^{(j)}}|_{s_0} = 3 \quad (\text{keep}), \\ 0 & \Rightarrow |\kappa_I \kappa_{I_1^{(j)}} \kappa_{I_2^{(j)}}|_{s_0} = 2 \quad (\text{discard}). \end{cases}$$

If one of the three pairwise intersections is 0, we compute $|\kappa_I \kappa_{I_1^{(j)}} \kappa_{I_2^{(j)}}|_{s_0}$ directly (or via short relations) and keep only those with level 3.

Double-coset identification via matrices: For each surviving ordered triple $\widehat{I} = (I, I_1^{(j)}, I_2^{(j)})$, the transformation data $\text{Trans}(\widehat{I})$ is given by the matrix representation M of $\kappa_I \kappa_{I_1^{(j)}} \kappa_{I_2^{(j)}}$ in the basis $\{e_0, \dots, e_{10}\}$. We identify two such matrices up to left/right multiplication by $W(A_9)$, which acts by permuting the indices 1, ..., 10 and fixes e_0 :

$$M_1 \approx M_2 \Leftrightarrow M_1 = \rho M_2 \sigma \quad \text{for some } \rho, \sigma \in W(A_9).$$

Concretely, left multiplication by ρ permutes rows corresponding to indices 1, ..., 10, and right multiplication by σ permutes columns corresponding to indices 1, ..., 10. We choose one representative in each double coset $W(A_9) \text{Trans}(\widehat{I}) W(A_9)$ and record the corresponding I . The resulting (finite) list yields T_3 .

Repeating the same procedure inductively produces T_{n+1} from T_n :

Inductive step $T_n \rightarrow T_{n+1}$. Given a representative $\widehat{I}' = (I_1, \dots, I_n) \in T_n$, adjoin $I \in T$ in front to form (I, \widehat{I}') . Filter by adjacency $|I \cap I_1| \in \{0, 1\}$; apply the level test using the relevant κ –relations (pair and triple lemmas) to ensure the s_0 –length is $n+1$; then identify double cosets via matrix representatives modulo left/right $W(A_9)$ –action as above. The surviving I ’s determine T_{n+1} . This procedure is straightforward to implement computationally. A SageMath implementation is provided in Appendix B.

3.2. Algebraic structure of the double coset. The set of double cosets $W(A_9) \backslash W(E_{10}) / W(A_9)$ does not itself carry a natural group structure. For $x, y \in W(E_{10})$, the product

$$(W(A_9)xW(A_9)) \cdot (W(A_9)yW(A_9))$$

is, in general, a finite *disjoint union* of double cosets, rather than a single one. However, the free abelian group $\mathbb{Z}[W(A_9) \backslash W(E_{10}) / W(A_9)]$ admits a natural associative algebra structure under convolution:

$$[W(A_9)xW(A_9)] * [W(A_9)yW(A_9)] := \sum_{z \in A_9 W A_9} m_{x,y}^z [W(A_9)zW(A_9)],$$

where each coefficient $m_{x,y}^z \in \mathbb{Z}_{\geq 0}$ counts the number of ways to factor elements of the product $(W(A_9)xW(A_9)) \cdot (W(A_9)yW(A_9))$ through the double coset $W(A_9)zW(A_9)$. This algebra is the *parabolic Hecke algebra* associated with $(W(E_{10}), W(A_9))$ at $q = 1$.

Let (W, S) be a Coxeter system and let $J \subset S$. Denote by W_J the standard parabolic subgroup generated by J . It is well known [2, Proposition 2.7(a)] that each double coset $W_J w W_J$ admits a unique element of minimal length (equivalently, minimal with respect to the Bruhat order). This follows from the general theory of parabolic decompositions and the exchange condition (see, e.g., [14, 15, 3, 24, 6, 12]). In our setting, K denotes the set of all such minimal double–coset representatives for $W(A_9) \backslash W(E_{10}) / W(A_9)$.

For each integer $n \geq 1$, set

$$K_n = \{ \kappa_{\widehat{I}} : \widehat{I} \in T_n \}, \quad K_0 = \{ \text{id} \}.$$

Then the union

$$K := \bigcup_{n \geq 0} K_n$$

forms a complete set of minimal–length double–coset representatives for

$$W(A_9) \backslash W(E_{10}) / W(A_9)$$

with respect to the s_0 –length filtration. Explicitly,

$$W(E_{10}) = \bigsqcup_{n \geq 0} \bigsqcup_{\kappa_{\widehat{I}} \in K_n} W(A_9) \kappa_{\widehat{I}} W(A_9),$$

and each element $\kappa_{\widehat{I}}$ has minimal possible s_0 –length within its double coset. Thus each Bruhat–minimal representative of $W(A_9) \backslash W(E_{10}) / W(A_9)$ can be identified with a unique element $\kappa_{\widehat{I}} \in K$. With this identification, we can endow K with a natural monoid structure via the Demazure product.

Demazure product. Let $K = \bigcup_{n \geq 0} K_n$ denote the set of minimal double–coset representatives for $W(A_9) \backslash W(E_{10}) / W(A_9)$. For $x, y \in K$, define the *Demazure product* \diamond by

$$x \diamond y := \min_{\leq_{\text{Bruhat}}} (K \cap W(A_9) x y W(A_9)),$$

that is, the unique Bruhat-minimal element in the double coset containing xy . Let

$$\pi_D: W(E_{10}) \longrightarrow K$$

be the projection sending each $x \in W(E_{10})$ to the unique minimal representative $\kappa_{\widehat{I}} \in K$ of the double coset containing x .

The associativity of the Demazure product and the monoid homomorphism property of π_D hold for arbitrary Coxeter systems; see Kazhdan–Lusztig [15], Dyer [12], and Deodhar [6]. For finite Coxeter groups, these results also appear in Geck–Pfeiffer [13, Chap. 8].

In particular, the set K of minimal double–coset representatives in $W(E_{10})$ is closed under the Demazure product \diamond , and

$$\pi_D(xy) = \pi_D(x) \diamond \pi_D(y), \quad x, y \in W(E_{10}).$$

Proposition 3.8. *The Demazure product \diamond on K is associative and has identity element $\text{id} \in K$. Moreover, the projection $\pi_D: W(E_{10}) \rightarrow K$ is a monoid homomorphism:*

$$\pi_D(xy) = \pi_D(x) \diamond \pi_D(y) \quad \text{for all } x, y \in W(E_{10}).$$

Proof. Each $\kappa \in K$ is the unique Bruhat-minimal representative of its double coset $W(A_9)\kappa W(A_9)$. The compatibility of double coset multiplication with Bruhat order ensures that the minimal representative of a product of double cosets is determined by the Demazure product \diamond . These properties follow from the general theory of Hecke monoids and parabolic Bruhat decompositions; see, e.g., Dyer [12, Thm. 2.4]. \square

This product endows K with a natural monoid structure, encoding the graded double–coset stratification of $W(E_{10})$, and will serve as the algebraic framework for the spectral and geometric analysis developed in the following sections.

4. THE s_0 -LEVEL FILTRATION OF $W(E_{10})$

We begin by introducing a natural stratification of $W(E_{10})$ determined by the distinguished generator s_0 . We write

$$\text{Conj}(W(E_{10})) := \{[\omega] \mid \omega \in W(E_{10})\}$$

for the set of conjugacy classes in $W(E_{10})$, where $[\omega] = \{x\omega x^{-1} \mid x \in W(E_{10})\}$. For a conjugacy class $[\omega] \in \text{Conj}(W(E_{10}))$, we define its s_0 -level by the function

$$h_{s_0}: \text{Conj}(W(E_{10})) \longrightarrow \mathbb{Z}_{\geq 0}, \quad h_{s_0}(\omega) := \min_{v \in [\omega]} |v|_{s_0}.$$

Thus $h_{s_0}(\omega)$ measures the smallest possible s_0 -length among all representatives of the class. This invariant partitions the set of conjugacy classes of $W(E_{10})$ according to their minimal interaction with the distinguished reflection s_0 .

We may now decompose the conjugacy set $\text{Conj}(W(E_{10}))$ into strata according to the s_0 -level:

$$\text{Conj}(W(E_{10})) = \bigsqcup_{k \geq 0} F_k, \quad F_k = \{[\omega] \in \text{Conj}(W(E_{10})) \mid h_{s_0}(\omega) = k\},$$

so that each F_k consists of the conjugacy classes whose representatives achieve minimal s_0 -length k . We refer to this partition as the s_0 -level decomposition of $W(E_{10})$.

If $\omega' \in W(E_{10})$ is conjugate to ω with $|\omega|_{s_0} = k$, then

$$|\omega'|_{s_0} \geq k.$$

Hence

$$\omega' \in \bigsqcup_{n \geq k} \bigsqcup_{\kappa_{\widehat{I}} \in K_n} W(A_9) \kappa_{\widehat{I}} W(A_9).$$

For each integer $n \geq 0$, let \mathcal{D}_n denote the union of double cosets corresponding to the representatives $\kappa_{\widehat{I}} \in K_n$:

$$\mathcal{D}_n := \bigsqcup_{\kappa_{\widehat{I}} \in K_n} W(A_9) \kappa_{\widehat{I}} W(A_9).$$

Thus \mathcal{D}_n collects all elements of $W(E_{10})$ whose minimal s_0 -length equals n . Using conjugacy in $W(E_{10})$, we can further decompose \mathcal{D}_n by the s_0 -level of the conjugacy class.

Since F_k denotes the set of conjugacy classes in $W(E_{10})$ represented by elements of s_0 -length k , we have

$$(4.1) \quad \mathcal{D}_n = \bigsqcup_{k \leq n} \mathcal{D}_{n,k}, \quad \mathcal{D}_{n,k} := \{ \omega \in \mathcal{D}_n : [\omega] \in F_k \}.$$

Geometrically, conjugation by elements of $W(A_9)$ corresponds to moving the reflection hyperplane associated with s_0 within the E_{10} Tits cone. The s_0 -level therefore measures the *depth* of the orbit in the hyperbolic direction, providing a natural stratification of $W(E_{10})$ by increasing geometric complexity.

Let $\rho(\cdot)$ denote the spectral radius of the linear action on $\text{span}\{e_0, \dots, e_{10}\}$. Since our representation is faithful and conjugation acts by similarity, ρ is a class function on $W(E_{10})$.

For $n \geq 0$ define the spectral set at s_0 -level n by

$$\Lambda_n := \{ \rho(\omega) : [\omega] \in F_n \}.$$

Equivalently, since F_n consists of conjugacy classes whose minimal representatives have s_0 -length n , we have

$$\Lambda_n = \{ \rho(\omega) : \omega \in \mathcal{D}_{n,n} \}.$$

More generally, for $k \leq n$ set

$$\text{Spec}(\mathcal{D}_{n,k}) := \{ \rho(\omega) : \omega \in \mathcal{D}_{n,k} \}.$$

Lemma 4.1. *For every $n \geq k$ one has*

$$\text{Spec}(\mathcal{D}_{n,k}) \subseteq \Lambda_k.$$

In particular,

$$\text{Spec}(\mathcal{D}_n) = \bigcup_{k \leq n} \text{Spec}(\mathcal{D}_{n,k}) \subseteq \bigcup_{k \leq n} \Lambda_k, \quad \text{and} \quad \Lambda_n = \text{Spec}(\mathcal{D}_{n,n}).$$

Proof. If $\omega \in \mathcal{D}_{n,k}$, then $[\omega] \in F_k$ by definition. Hence there exists ω' conjugate to ω with $|\omega'|_{s_0} = k$, i.e. $\omega' \in \mathcal{D}_k$. Since ρ is conjugacy invariant, $\rho(\omega) = \rho(\omega') \in \Lambda_k$, proving $\text{Spec}(\mathcal{D}_{n,k}) \subseteq \Lambda_k$. The remaining assertions are immediate from $\mathcal{D}_n = \bigsqcup_{k \leq n} \mathcal{D}_{n,k}$ and the definition of Λ_n . \square

Consequently, *new* spectral radii that first appear at level n lie in $\Lambda_n = \text{Spec}(\mathcal{D}_{n,n})$; elements of $\mathcal{D}_{n,k}$ with $k < n$ can only contribute spectral radii already present at level k .

4.1. Spectral refinement and growth graph of minimal representatives. The spectral set Λ_n can be refined using the minimal representatives in T_n . For each $\widehat{I} \in T_n$, define

$$\Lambda_n(\widehat{I}) := \{ \rho(\omega) : \omega \in \mathcal{D}_{n,n} \text{ and } \omega \in W(A_9) \kappa_{\widehat{I}} W(A_9) \}.$$

Define an equivalence relation on T_n by

$$\widehat{I} \sim \widehat{J} \iff \kappa_{\widehat{I}} = \kappa_{\widehat{J}} \text{ or } \kappa_{\widehat{I}} = \kappa_{\widehat{J}}^{-1}.$$

Since $\rho(\omega) = \rho(\omega^{-1})$ (the characteristic polynomial is a Salem polynomial times cyclotomic factors), we have $\Lambda_n(\widehat{I}) = \Lambda_n(\widehat{J})$ whenever $\widehat{I} \sim \widehat{J}$. Thus

$$\Lambda_n = \bigcup_{[\widehat{I}] \in T_n/\sim} \Lambda_n(\widehat{I}),$$

a (generally non-disjoint) cover of Λ_n by source classes modulo inversion.

s_0 -growth graph and the spectral growth filtration. Since the sets T_n were constructed recursively from T_{n-1} by adjoining admissible triples (cf. Section 3.1.2), the family $\{T_n/\sim\}_{n \geq 0}$ forms a directed acyclic structure: each vertex $[\widehat{I}] \in T_n/\sim$ is connected by directed edges to the class of $(n+1)$ -tuples in T_{n+1}/\sim that extend it. We refer to this directed system as the s_0 -growth graph of minimal representatives. Although different branches may merge (two distinct extensions may lead to the same double coset), the overall graph remains acyclic and records how new minimal representatives—and hence new spectral contributions—arise from lower levels.

For each directed path

$$[\widehat{I}^{(1)}] \longrightarrow [\widehat{I}^{(2)}] \longrightarrow \cdots \longrightarrow [\widehat{I}^{(n)}], \quad [\widehat{I}^{(m)}] \in T_m/\sim,$$

in the growth graph, we obtain a sequence of spectral subsets

$$\Lambda_1(\widehat{I}^{(1)}), \Lambda_2(\widehat{I}^{(2)}), \dots, \Lambda_n(\widehat{I}^{(n)}),$$

recording how the spectral radii evolve along the recursive construction of minimal double-coset representatives. We refer to this sequence as the *spectral growth filtration*. It provides a combinatorial framework for tracing how new spectral radii first appear in Λ_n as n increases, and how they propagate through the overlapping branches of the s_0 -growth graph.

Remark 4.2. *The spectral growth filtration traces the appearance of new spectral values level by level, rather than forming a nested inclusion of sets. In particular, each $\Lambda_n(\widehat{I})$ records the spectral radii arising for the first time at s_0 -level n . The cumulative spectra*

$$\Lambda_{\leq n} := \bigcup_{k \leq n} \Lambda_k$$

do form a nested family $\Lambda_{\leq 1} \subseteq \Lambda_{\leq 2} \subseteq \dots$, reflecting the overall accumulation of spectral radii across levels. Thus, while the sequence $\{\Lambda_k(\widehat{I}^{(k)})\}_{k \geq 1}$ captures the emergence dynamics of individual spectral contributions, the nested system $\{\Lambda_{\leq n}\}_{n \geq 1}$ describes their global spectral aggregation.

Using the recursive construction from Section 3.1.2, Figure 2 illustrates the s_0 -growth graph for small s_0 -levels as a branching graph. Each node represents the newly adjoined triple along a directed path. As shown in Figure 2, s_0 -growth graph is a rooted directed acyclic graph. For example, the leftmost downward path in Figure 2 corresponds to

$$(1, 2, 3) \longrightarrow (1, 4, 5) \longrightarrow (1, 6, 7),$$

which in terms of ordered sets of triples gives

$$\{(1, 2, 3)\} \in T_1/\sim \longrightarrow \{(1, 4, 5), (1, 2, 3)\} \in T_2/\sim \longrightarrow \{(1, 6, 7), (1, 4, 5), (1, 2, 3)\} \in T_3/\sim.$$

Two different nodes in the branching graph can merge. For example,

$$\{(5, 6, 7), (1, 4, 5), (1, 2, 3)\} = \{(1, 5, 7), (4, 5, 6), (1, 2, 3)\} \in T_3/\sim.$$

Hence there are merging branches emanating from the two nodes $(1, 4, 5)$ and $(4, 5, 6)$ on the second level in Figure 2. To simplify the diagram, we label each vertex by the triple appearing along the leftmost downward directed path. In particular, the next node is recorded as $(5, 6, 7)$ (rather than $(1, 5, 7)$) to avoid duplication and confusion.

In this way, the branching graph provides a combinatorial visualization of the recursive generation of minimal double–coset representatives and their associated spectral contributions.

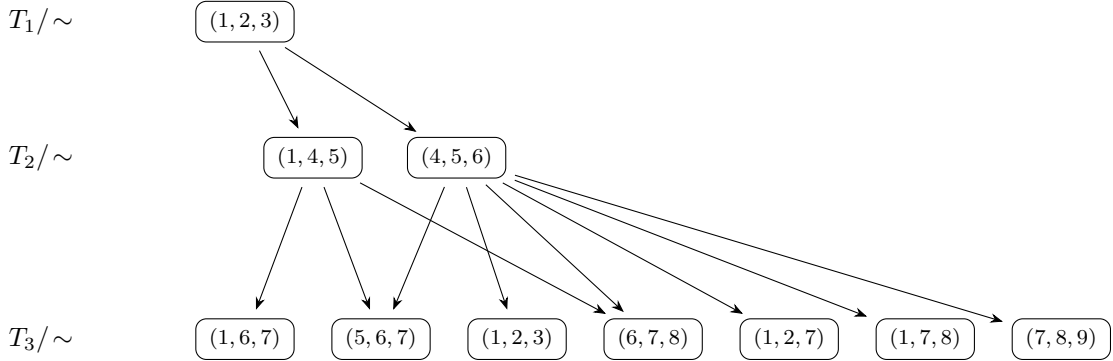


FIGURE 2. Branching graph for $T_1/\sim \rightarrow T_2/\sim \rightarrow T_3/\sim$. Each directed edge represents the extension process in which a new ordered set of triples \hat{I} is obtained by adjoining the triple indicated at the end of the branch as the first triple in the sequence. For clarity, only the leftmost directed paths are shown, so that each node is labeled by the triples appearing along that path.

We summarize our discussion in Section 3 and Section 4 in the following theorem:

Theorem 4.3 (Triple-Labeled Graph Structure of Minimal Representatives). *Let $\mathcal{D}_{n,n}$ denote the set of elements in $W(E_{10})$ of s_0 -level n (as defined in (4.1)), and let $K \subset W(E_{10})$ be the set of Bruhat-minimal representatives of double cosets $W(A_9) \backslash W(E_{10}) / W(A_9)$.*

Then:

- (1) *Each $\kappa \in K \cap \mathcal{D}_{n,n}$ is uniquely determined by an ordered n -tuple of triples from*

$$T := \{\{i, j, k\} \subset \{1, \dots, 10\} : 1 \leq i < j < k \leq 10\}.$$

- (2) *There exists a rooted directed acyclic graph (DAG) \mathcal{G} , whose depth- n nodes correspond bijectively to a finite inductively defined subset $T_n \subset T^n$, such that each directed path of length n encodes the recursive construction of a minimal double coset representative $\kappa \in \mathcal{D}_{n,n}$.*

5. SPECTRAL RADII VIA THE HILBERT METRIC

The matrix representation of each $\omega \in W(E_{10})$ in the basis $\{\mathbf{e}_0, \mathbf{e}_1, \dots, \mathbf{e}_{10}\}$ defines the geometric representation

$$\sigma : W(E_{10}) \longrightarrow O(V),$$

where $V \subset \mathbb{R}^{1,10}$ defined in Section 2. The dual action on V^* is given by

$$\langle \omega(f), \omega(v) \rangle = \langle f, v \rangle, \quad \omega \in W(E_{10}), f \in V^*, v \in V,$$

here $\langle f, v \rangle$ denotes the natural pairing of $f \in V^*$ with $v \in V$

Each simple reflection $s_i \in S$ acts as the reflection through the hyperplane orthogonal to the simple root

$$\alpha_0 = \mathbf{e}_0 - \mathbf{e}_1 - \mathbf{e}_2 - \mathbf{e}_3, \quad \alpha_i = \mathbf{e}_i - \mathbf{e}_{i+1} \quad (i = 1, \dots, 9).$$

For each α_i let

$$H_i := \{f \in V^* : \langle f, \alpha_i \rangle = 0\},$$

with corresponding open half-spaces

$$H_i^\pm := \{f \in V^* : \pm \langle f, \alpha_i \rangle > 0\}.$$

The fundamental chamber is the closed convex cone

$$F := \{ f \in V^* : \langle f, \alpha_i \rangle \geq 0 \text{ for all } i = 0, \dots, 9 \}.$$

The *Tits cone* of $W(E_{10})$ is the orbit

$$U := \bigcup_{\omega \in W(E_{10})} \omega(F),$$

on which $W(E_{10})$ acts properly by linear isometries.

Hilbert metric. If $\mathcal{C} \subset V^*$ is a proper open convex cone and $x \neq y \in \mathcal{C}$, let $a, b \in \partial\mathcal{C}$ be the two intersection points of the line \overline{xy} with $\partial\mathcal{C}$ ordered a, x, y, b ; the Hilbert distance is

$$d_{\mathcal{C}}(x, y) := \log[a, x, y, b],$$

where $[a, x, y, b] = \frac{|ax||yb|}{|ay||xb|}$ is the projective cross ratio.

To follow McMullen's notation [20], let K denote the closure of the Tits cone U , and let K° denote its interior. By McMullen, the group $W(E_{10})$ acts discretely and isometrically for the Hilbert metric on the convex cone K° , with $X = F \cap K^\circ$ as a fundamental domain. Moreover, the spectral radius of ω is related to its Hilbert translation length as follows:

Proposition 5.1 ([20, Cor. 3.5]). *For each $\omega \in W(E_{10})$,*

$$\log \rho(\omega) = \inf_{x \in K^\circ} d_K(x, \omega x),$$

where d_K denotes the Hilbert metric on K .

One of the key advantages of the Hilbert metric on K is that it satisfies the triangle inequality: for all $x, y, z \in K^\circ$,

$$d_K(x, z) \leq d_K(x, y) + d_K(y, z).$$

This immediately implies a submultiplicativity property for spectral radius.

Proposition 5.2. *For $\omega_1, \omega_2 \in W(E_{10})$,*

$$\rho(\omega_1 \omega_2) \leq \rho(\omega_1) \rho(\omega_2).$$

Proof. By the triangle inequality,

$$d_K(x, \omega_1 \omega_2 x) \leq d_K(x, \omega_2 x) + d_K(\omega_2 x, \omega_1(\omega_2 x)).$$

Taking the infimum over all $x \in K^\circ$ on the left-hand side gives

$$\inf_{x \in K^\circ} d_K(x, \omega_1 \omega_2 x) \leq d_K(x, \omega_2 x) + d_K(\omega_2 x, \omega_1 \omega_2 x).$$

Again, taking the infimum over all $x \in K^\circ$ to both terms separately on the right hand side, we have

$$\inf_{x \in K^\circ} d_K(x, \omega_1 \omega_2 x) \leq \inf_{x \in K^\circ} d_K(x, \omega_2 x) + \inf_{y \in K^\circ} d_K(y, \omega_1 y).$$

Applying Proposition 5.1 to each term gives

$$\log \rho(\omega_1 \omega_2) \leq \log \rho(\omega_1) + \log \rho(\omega_2),$$

which is equivalent to the desired inequality. \square

Let $\omega \in W(E_{10})$ be given by a reduced word

$$\omega = g_1 g_2 \cdots g_m, \quad g_i \in S.$$

We say that ω' is a *subword* of ω if there exist indices $1 \leq i_1 < i_2 < \cdots < i_k \leq m$ such that $\omega' = g_{i_1} g_{i_2} \cdots g_{i_k}$.

Let $\pi : K^\circ \rightarrow X$ denote the natural projection sending each $x \in K^\circ$ to the unique point $\pi(x) \in X$ in its $W(E_{10})$ -orbit. By McMullen [20, Section 4], one obtains the following useful conclusion, stated here in a form adapted to our setting.

Proposition 5.3 ([20, Section 4]). *Suppose ω' is a subword of ω . Then*

$$\rho(\omega') \leq \rho(\omega).$$

5.1. Spectral Emergence Sequence. Let $\{\Lambda_k(\widehat{I}^{(k)})\}_{k \geq 1}$ denote the sequence of spectral subsets associated with a directed path in the s_0 -growth graph (cf. Section 4.1). This sequence records the emergence of new spectral values as admissible triples are successively adjoined.

(1) The initial node corresponds to

$$\widehat{I}^{(1)} = \{(1, 2, 3)\} \in T_1.$$

(2) For each $k \geq 2$, the ordered set of triples $\widehat{I}^{(k)}$ is obtained by adjoining a new triple $J \in T$ to the beginning of $\widehat{I}^{(k-1)} = \{I_1, \dots, I_{k-1}\}$:

$$\widehat{I}^{(k)} = \{J, I_1, \dots, I_{k-1}\}.$$

Equivalently, $\widehat{I}^{(k)}$ extends $\widehat{I}^{(k-1)}$ by one admissible triple in the recursive construction of T_k from T_{k-1} (see Section 3.1.2).

(3) For each $k \geq 1$, let $\kappa_{\widehat{I}^{(k)}}$ denote the corresponding product of reflections. It is the unique minimal representative in its double coset

$$W(A_9) \kappa_{\widehat{I}^{(k)}} W(A_9).$$

(4) The associated spectral subset $\Lambda_k(\widehat{I}^{(k)})$ consists of the spectral radii of all elements $\omega \in W(E_{10})$ that belong to the intersection

$$\mathcal{D}_{k,k} \cap W(A_9) \kappa_{\widehat{I}^{(k)}} W(A_9),$$

that is, those elements whose minimal s_0 -length equals k and which lie in the double coset of $\kappa_{\widehat{I}^{(k)}}$.

The sequence $\{\Lambda_k(\widehat{I}^{(k)})\}_{k \geq 1}$ thus describes the successive appearance of spectral radii along a fixed directed path in the s_0 -growth graph, and forms the analytic counterpart of the combinatorial branching structure developed in Section 4.1. Define

$$\mathcal{D}_k(\widehat{I}^{(k)}) := \mathcal{D}_{k,k} \cap W(A_9) \kappa_{\widehat{I}^{(k)}} W(A_9),$$

so that

$$\Lambda_k(\widehat{I}^{(k)}) = \{\rho(\omega) : \omega \in \mathcal{D}_k(\widehat{I}^{(k)})\}.$$

Lemma 5.4. *For each $\widehat{I}^{(k)} \in T_k$, there exist elements $\omega_k, \omega'_k \in \mathcal{D}_k(\widehat{I}^{(k)})$ such that*

$$\rho(\omega_k) = \max \Lambda_k(\widehat{I}^{(k)}) \quad \text{and} \quad \rho(\omega'_k) = \min \Lambda_k(\widehat{I}^{(k)}).$$

Moreover, the element ω_k with maximal spectral radius is conjugate to one of the form $\kappa_{\widehat{I}^{(k)}} \eta_k$, where $\eta_k \in W(A_9)$:

$$[\omega_k] = [\kappa_{\widehat{I}^{(k)}} \eta_k].$$

Proof. Since each double coset $W(A_9) \kappa_{\widehat{I}^{(k)}} W(A_9)$ is finite, $\Lambda_k(\widehat{I}^{(k)})$ attains both a maximum and a minimum. Let ω_k be the element achieving the maximal spectral radius. Because ω_k has s_0 -length k and $\kappa_{\widehat{I}^{(k)}}$ is the unique minimal representative of its double coset, there exists $\eta_k \in W(A_9)$ such that $[\omega_k] = [\kappa_{\widehat{I}^{(k)}} \eta_k]$. \square

Lemma 5.5. *Let $\widehat{I}^{(k)} = \{J, I_1, \dots, I_{k-1}\}$. Then for every $\omega \in \mathcal{D}_k(\widehat{I}^{(k)})$ there exists $\sigma \in W(A_9)$ such that*

$$[\omega] = [\sigma \kappa_J \omega_{k-1}],$$

where ω_{k-1} is the element of $\mathcal{D}_{k-1}(\widehat{I}^{(k-1)})$ with maximal spectral radius. Moreover, $\sigma \kappa_J \omega_{k-1}$ is expressed in reduced word form.

Proof. Let ω_{k-1} and $\eta_{k-1} \in W(A_9)$ be as in Lemma 5.4, so that $[\omega_{k-1}] = [\kappa_{\widehat{I}^{(k-1)}} \eta_{k-1}]$. If $\omega \in \mathcal{D}_k(\widehat{I}^{(k)})$, then $\omega = \alpha \kappa_J \kappa_{\widehat{I}^{(k-1)}} \beta$ for some $\alpha, \beta \in W(A_9)$. Conjugating by $\beta^{-1} \eta_{k-1}$ gives

$$[\omega] = [\eta_{k-1}^{-1} \beta \alpha \kappa_J \kappa_{\widehat{I}^{(k-1)}} \eta_{k-1}].$$

Since $\kappa_J \kappa_{\widehat{I}^{(k-1)}}$ is the unique minimal element in its double coset, we may reduce the prefactor $\eta_{k-1}^{-1} \beta \alpha$ to a single $\sigma \in W(A_9)$, obtaining

$$[\omega] = [\sigma \kappa_J \omega_{k-1}].$$

□

Proposition 5.6. *Let $\{\Lambda_k(\widehat{I}^{(k)})\}_{k \geq 1}$ be the sequence of spectral subsets associated with a directed path in the s_0 -growth graph. Then for every $\rho \in \Lambda_k(\widehat{I}^{(k)})$,*

$$\max \Lambda_{k-1}(\widehat{I}^{(k-1)}) \leq \rho \leq \min \Lambda_{k+1}(\widehat{I}^{(k+1)}).$$

Proof. If $\rho \in \Lambda_k(\widehat{I}^{(k)})$, then there exists $\omega \in \mathcal{D}_k(\widehat{I}^{(k)})$ with $\rho = \rho(\omega)$. By Lemma 5.5, a conjugate of ω_{k-1} appears as a subword of ω . Since the spectral radius is invariant under conjugation, Proposition 5.3 implies

$$\rho \geq \rho(\omega_{k-1}) = \max \Lambda_{k-1}(\widehat{I}^{(k-1)}).$$

Applying the same argument to $\Lambda_{k+1}(\widehat{I}^{(k+1)})$ yields the upper bound, completing the proof. □

Proposition 5.6 reveals that the spectral evolution along any directed path in the s_0 -growth graph is *monotone and constrained*. Each new level k inherits its spectral range from the previous level, bounded below by $\max \Lambda_{k-1}(\widehat{I}^{(k-1)})$ and above by $\min \Lambda_{k+1}(\widehat{I}^{(k+1)})$. In geometric terms, as one adjoins successive reflections κ_J in the recursive construction, the corresponding action on the Tits cone expands the spectral radius only within a controlled interval. This monotone interlacing of spectral sets reflects the ordered structure of minimal double-coset representatives and anticipates the continuous scaling behavior governed by the Hilbert metric.

Theorem 5.7 (Spectral Monotonicity). *Let $\{\Lambda_k(\widehat{I}^{(k)})\}_{k \geq 1}$ be the sequence of spectral subsets associated with a directed path in the s_0 -growth graph. Then the sequences of minima and maxima are non-decreasing in s_0 -level k :*

$$\min \Lambda_k(\widehat{I}^{(k)}) \leq \min \Lambda_{k+1}(\widehat{I}^{(k+1)}), \quad \max \Lambda_k(\widehat{I}^{(k)}) \leq \max \Lambda_{k+1}(\widehat{I}^{(k+1)}) \quad \text{for all } k \geq 1.$$

Proof. This follows immediately from Proposition 5.6, which ensures that

$$\max \Lambda_k(\widehat{I}^{(k)}) \leq \min \Lambda_{k+1}(\widehat{I}^{(k+1)}).$$

□

5.2. **Levelwise Spectral Envelopes.** For the initial node $\widehat{I}^{(1)} = \{(1, 2, 3)\}$,

$$\Lambda_1([\widehat{I}^{(1)}]) = \{\rho(\omega) : \omega \in \mathcal{D}_{1,1} \cap W(A_9) \kappa_{\widehat{I}^{(1)}} W(A_9)\}.$$

Since the double coset $W(A_9) \kappa_{\widehat{I}^{(1)}} W(A_9)$ is finite, the set $\Lambda_1([\widehat{I}^{(1)}])$ attains both a maximum and a minimum > 1 .¹ Define

$$\begin{aligned} \text{Max}_1([\widehat{I}^{(1)}]) &:= \max \Lambda_1([\widehat{I}^{(1)}]), \\ \text{Min}_1([\widehat{I}^{(1)}]) &:= \min \{\rho \in \Lambda_1([\widehat{I}^{(1)}]) : \rho > 1\}. \end{aligned}$$

By McMullen [20, Thm. 4.1], the minimum $\text{Min}_1([\widehat{I}^{(1)}])$ equals *Lehmer's number* $\lambda_L \approx 1.17628$, the largest real root of the reciprocal polynomial

$$L(t) = t^{10} + t^9 - t^7 - t^6 - t^5 - t^4 - t^3 + t + 1.$$

By direct computation, the maximum $\text{Max}_1([\widehat{I}^{(1)}]) = M_1$ is the largest real root of

$$P(t) = t^{10} - t^9 - t^8 + t^7 - t^5 + t^3 - t^2 - t + 1.$$

In fact, there are exactly 11 distinct spectral radii > 1 in $\Lambda_1([\widehat{I}^{(1)}])$. Table 1 lists these values (rounded), together with their degrees and a compact encoding of the *reciprocal* minimal polynomials: for a reciprocal polynomial of even degree $2d$, we list the first $d+1$ coefficients (a_0, \dots, a_d) , since the remaining d are determined by palindromy.

k	spectral radius ρ_k	degree	reciprocal coeffs $(a_0, \dots, a_{d/2})$
1	1.17628	10	1, 1, 0, -1, -1, -1
2	1.21639	10	1, 0, 0, 0, -1, -1
3	1.26123	10	1, 0, -1, 0, 0, -1
4	1.28064	8	1, 0, 0, -1, -1
5	1.29349	10	1, 0, -1, -1, 0, 1
6	1.35098	10	1, -1, 0, 0, -1, 1
7	1.36000	8	1, -1, 1, -2, 1
8	1.38364	10	1, -1, 0, -1, 1, -1
9	1.40127	6	1, 0, -1, -1
10	1.42501	8	1, -1, 0, -1, 1
11	1.43100	10	1, -1, -1, 1, 0, -1

TABLE 1. Spectral radii in $\Lambda_1([\widehat{I}^{(1)}])$. Each row corresponds to the largest real root of a reciprocal polynomial determined by the listed first half of coefficients.

For higher levels $n \geq 2$, we aggregate the nodewise extrema over the equivalence classes T_n/\sim . For each node class $[\widehat{I}] \in T_n/\sim$, define

$$\begin{aligned} \text{Max}_n([\widehat{I}]) &:= \max \Lambda_n([\widehat{I}]), \\ \text{Min}_n([\widehat{I}]) &:= \min \Lambda_n([\widehat{I}]). \end{aligned}$$

If $[\widehat{J}_1] \in T_{n-1}/\sim$ and $[\widehat{J}_2] \in T_{n+1}/\sim$ are connected to $[\widehat{I}] \in T_n/\sim$ by a directed path

$$[\widehat{J}_1] \longrightarrow [\widehat{I}] \longrightarrow [\widehat{J}_2],$$

then Proposition 5.6 yields

$$\text{Max}_{n-1}([\widehat{J}_1]) \leq \text{Min}_n([\widehat{I}]) \leq \text{Max}_n([\widehat{I}]) \leq \text{Min}_{n+1}([\widehat{J}_2]).$$

¹We exclude $\rho = 1$, which arises from elliptic or parabolic elements through cyclotomic factors.

We now define the *levelwise spectral envelopes*

$$\begin{aligned} M_n &:= \min_{[\widehat{I}] \in T_n/\sim} \text{Max}_n([\widehat{I}]), & \text{("bottleneck maximum" at level } n\text{),} \\ m_n &:= \max_{[\widehat{I}] \in T_n/\sim} \text{Min}_n([\widehat{I}]), & \text{("bottleneck minimum" at level } n\text{).} \end{aligned}$$

By Proposition 5.6, both sequences (m_n) and (M_n) are nondecreasing, and every $\rho \in \Lambda_n$ lies in the global spectral band

$$m_n \leq \rho \leq M_n.$$

Since each level T_n/\sim is finite, we can bound the levelwise envelopes via the pathwise inequalities:

$$M_{n-1} \leq m_n \leq M_n \quad (n \geq 2),$$

where

$$M_{n-1} = \min_{[\widehat{J}] \in T_{n-1}/\sim} \text{Max}_{n-1}([\widehat{J}]), \quad m_n = \max_{[\widehat{I}] \in T_n/\sim} \text{Min}_n([\widehat{I}]).$$

In particular, M_{n-1} provides a computable lower threshold for the level- n spectrum: every $\rho \in \Lambda_n$ satisfies $\rho \geq M_{n-1}$. Thus, by enumerating T_{n-1}/\sim and computing the nodewise maxima Max_{n-1} , we obtain an effective lower cutoff for Λ_n . Conversely, evaluating the nodewise maxima at level n yields M_n , an upper envelope for Λ_n .

Theorem 5.8 (Spectral Exhaustion Theorem). *For every $C > 1$, there exists an integer $N \geq 1$ such that*

$$\{\rho(\omega) \in \mathbb{R} : \omega \in W(E_{10}), \rho(\omega) \leq C\} \subset \bigcup_{n \leq N} \Lambda_n.$$

Proof. By Theorem 5.7, the level-wise spectral envelopes satisfy

$$m_1 \leq m_2 \leq \cdots \leq m_n \leq \cdots, \quad \text{with } \lim_{n \rightarrow \infty} m_n = \infty.$$

Hence, for any fixed $C > 1$, there exists N such that $m_N > C$, which implies that all spectral radii $\leq C$ must appear in some Λ_n for $n \leq N$. \square

In terms of computation, it is nontrivial to determine whether a given $\omega \in W(A_9)\kappa_{\widehat{I}}W(A_9)$, with $[\widehat{I}] \in T_n/\sim$, belongs to the s_0 -level stratum F_n . To overcome this challenge, we compute a larger superset

$$\tilde{\Lambda}_n := \{\rho(\omega) : \omega \in W(A_9)\kappa_{\widehat{I}}W(A_9), [\widehat{I}] \in T_n/\sim\}.$$

Since $m_n \in [M_{n-1}, M_n]$, this superset $\tilde{\Lambda}_n$ suffices to capture all spectral radii in Λ_n up to the lower bound M_{n-1} .

To understand how new spectral values emerge across successive s_0 -levels, we define the extremal emerging radii at level n :

$$\tilde{m}_n := \min(\tilde{\Lambda}_n \setminus \tilde{\Lambda}_{n-1}), \quad M_n := \max \tilde{\Lambda}_n.$$

This perspective clarifies the spectral growth process. As an example, we illustrate the levelwise spectral envelopes for small n in Table 2.

Notice that \tilde{m}_3 is numerically slightly smaller than M_2 ; this occurs because \tilde{m}_3 and M_2 are drawn from distinct directed paths in the s_0 -growth graph. Let $\omega_{\max} \in \mathcal{D}_{1,1}$ such that $\rho(\omega_{\max}) = M_1$. Then by the monoid structure of K given in Proposition 3.8, we have $\omega_{\max}^k \in \mathcal{D}_{k,k}$. Since $\rho(\omega^k) = \rho(\omega)^k$, $k \geq 1$, from Proposition 5.2, we have

Lemma 5.9. *For each $k \geq 1$,*

$$M_k = M_1^k.$$

For other extreme values, our computations reveal the empirical inequalities

$$\tilde{m}_k < M_{k-1} \quad \text{and} \quad \tilde{m}_k \approx \delta^{k-2} M_{k-1}, \quad k \geq 3,$$

where $\delta := \tilde{m}_3/M_2 \approx 0.9335$. Here “ \approx ” denotes numerical proximity rather than an established asymptotic equivalence. This scaling behavior suggests that the emergence of new spectral radii is geometrically separated at higher levels. Such exponential separation is reminiscent of displacement growth in Hilbert geometry; compare McMullen’s metric perspective in [20].

\tilde{m}_i, M_i	spectral radius ρ_k	degree	reciprocal coeffs $(a_0, \dots, a_{d/2})$
\tilde{m}_1	1.17628	10	1, 1, 0, -1, -1, -1
M_1	1.43100	10	1, -1, -1, 1, 0, -1
\tilde{m}_2	1.45799	8	1, 0, -1, -1, 0
M_2	2.04776	10	1, -3, 3, -3, 2, -1
\tilde{m}_3	1.91113	10	1, 0, -2, -2, -1, -1
M_3	2.93035	10	1, -1, -4, -5, 0, 2
\tilde{m}_4	2.56366	8	1, -1, -2, -3, -4
M_4	4.19334	10	1, -3, -5, 1, -2, -9
\tilde{m}_5	3.21255	8	1, -1, -4, -7, -7
M_5	6.00067	10	1, -6, -1, 6, 0, -1

TABLE 2. Levelwise spectral envelopes. Each entry corresponds to the largest real root of a reciprocal polynomial determined by the listed first half of coefficients.

These bounds enable complete enumeration of minimal polynomials for $\rho \in \Lambda_n$ below a given threshold. To focus on new spectral contributions, we consider only *primitive* Salem numbers, i.e., those for which no positive root $\rho^{1/k}$ lies in $\cup_n \Lambda_n$ for any $k > 1$.

Let $\hat{\Lambda}_n$ denote the set of newly emerged primitive Salem numbers at level n :

$$\hat{\Lambda}_n := \{\rho \in \tilde{\Lambda}_n \setminus \bigcup_{k < n} \tilde{\Lambda}_k : \rho \text{ is primitive.}\}.$$

In Table 1, the eighth Salem number is not primitive. The first Salem number, ρ_1 , is Lehmer’s number—the largest real root of the polynomial

$$t^{10} + t^9 - t^7 - t^6 - t^5 - t^4 - t^3 + t + 1.$$

The minimal polynomial of ρ_1^2 is given by

$$t^{10} - t^9 - t^7 + t^6 - t^5 + t^4 - t^3 - t + 1,$$

which shows that $\rho_8 = \rho_1^2$. Thus, the number of primitive Salem numbers at level one is $|\hat{\Lambda}_1| = 10$.

Similarly, by checking the minimal polynomials of powers of Salem numbers, we find $|\hat{\Lambda}_2| = 37$, $|\hat{\Lambda}_3| = 180$, $|\hat{\Lambda}_4| = 866$ and $|\hat{\Lambda}_5| = 4100$.

We include a complete list of all newly emerged primitive Salem numbers in $\hat{\Lambda}_2$ in Appendix A, along with the first 50 elements of $\hat{\Lambda}_3$. The full lists of primitive Salem numbers in $\hat{\Lambda}_n$, $n = 3, 4, 5$ are available in <https://www.math.fsu.edu/~kim/publication.html>.

Remark 5.10. *The growth of $\hat{\Lambda}_n$ appears to be exponential. We observe:*

$$\frac{|\hat{\Lambda}_2|}{|\hat{\Lambda}_1|} = \frac{37}{10} = 3.7, \quad \frac{|\hat{\Lambda}_3|}{|\hat{\Lambda}_2|} = \frac{180}{37} \approx 4.86, \quad \frac{|\hat{\Lambda}_4|}{|\hat{\Lambda}_3|} = \frac{866}{180} \approx 4.81, \quad \frac{|\hat{\Lambda}_5|}{|\hat{\Lambda}_4|} = \frac{4100}{866} \approx 4.73.$$

This suggests the heuristic:

$$|\hat{\Lambda}_{n+1}| \approx \eta_n \cdot |\hat{\Lambda}_n|, \quad \eta_n \approx 4 - (n-1)/10 \quad \text{for sufficiently large } n.$$

To gain further insight into the spectral density, we study the spacing between consecutive newly emerging Salem numbers in

$$\tilde{\Lambda}_n^{new} := \tilde{\Lambda}_n \setminus \bigcup_{k < n} \tilde{\Lambda}_k.$$

Let Gap_n denote the set of absolute differences between successive elements of $\tilde{\Lambda}_n^{new}$. From computation, we observe:

n	Average of Gap_n	Standard Deviation of Gap_n
1	0.0255	0.0168
2	0.0123	0.0081
3	0.0050	0.0051
4	0.0018	0.0030
5	0.0007	0.0024

TABLE 3. Levelwise Gap distribution.

Moreover, the average gap appears to decay exponentially, as shown in Figure 3. This suggests no arithmetic obstruction to accumulation—another indication of the fractal-like density of spectral radii within the Tits cone.

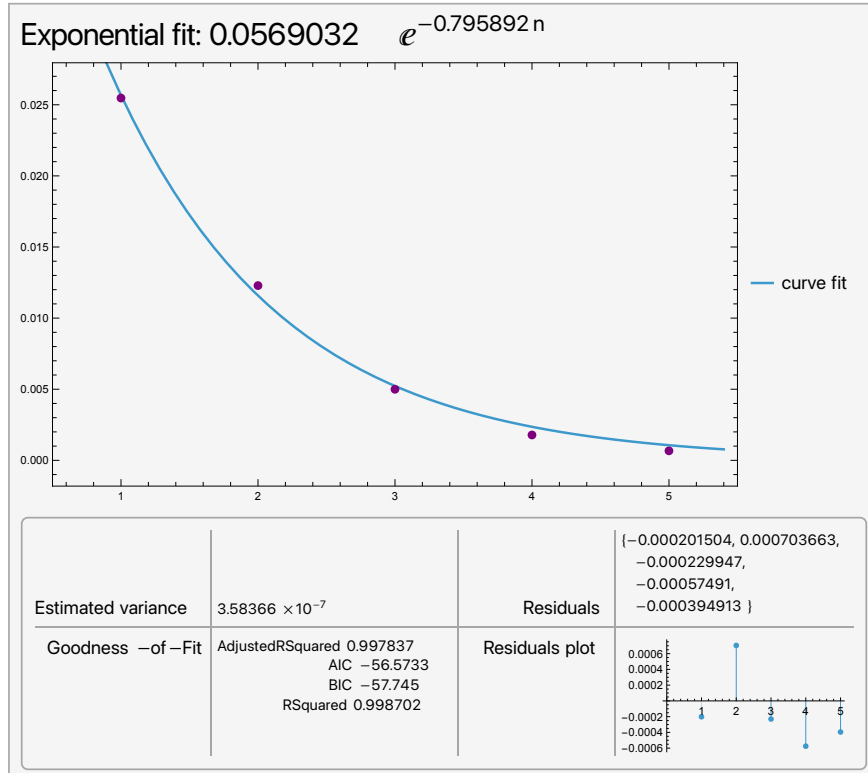


FIGURE 3. Exponential decay fit to the average gaps in Gap_n between newly emerged Salem numbers in $\tilde{\Lambda}_n^{new}$. Purple dots show observed means; the curve is a best-fit exponential regression obtained using Mathematica.

5.3. Hilbert–Metric Interpretation of Levelwise Growth. The spectral envelopes (m_n, M_n) introduced in Section 5.2 reflect the exponential growth rates of elements in $W(E_{10})$ measured by their s_0 –length. We now interpret this growth geometrically in terms of the Hilbert metric on the Tits cone.

Let $\mathcal{C} \subset V$ be the Tits cone of $W(E_{10})$, and let $\Omega \subset \mathbf{P}(V)$ denote its projectivization. Choose an affine slice of Ω intersecting the interior of the fundamental chamber in a bounded convex domain, so that the *Hilbert metric* d_K is well defined on Ω . Fix a basepoint x in the interior of the fundamental chamber.

For $\omega \in W(E_{10})$, define its *Hilbert displacement* at a basepoint x by

$$\delta_x(\omega) := d_K(x, \omega \cdot x),$$

where d_K denotes the Hilbert metric on the interior K° of the Tits cone. The *Hilbert translation length* of ω is

$$\ell_K(\omega) := \inf_{y \in K^\circ} d_K(y, \omega \cdot y).$$

By McMullen [20, Cor. 3.5], one has $\ell_K(\omega) = \log \rho(\omega)$.

Since each reflection in $W(E_{10})$ acts projectively on Ω by a cone–preserving linear transformation, the displacement $\delta(\omega)$ measures how far the element ω moves the chamber in the hyperbolic direction determined by s_0 . Note that $\delta_x(\omega)$ depends on the basepoint, while $\ell_K(\omega)$ is a conjugation-invariant lower bound.

For each level $n \geq 1$, define the levelwise displacement bounds

$$t_n := \inf\{\delta(\omega) : \omega \in \mathcal{D}_{n,n}\}, \quad T_n := \sup\{\delta(\omega) : \omega \in \mathcal{D}_{n,n}\}.$$

Then the Hilbert balls

$$B_n := B_K(x, t_n)$$

form a nested family $B_1 \subseteq B_2 \subseteq \dots$, whose union fills Ω . Moreover, by construction, the orbit points $\omega \cdot x$ with $\omega \in \mathcal{D}_{n,n}$ all lie outside $B_K(x, t_n - \varepsilon)$ for any $\varepsilon > 0$; that is, level n elements appear precisely beyond the Hilbert radius t_n .

Theorem 5.11 (Hilbert Ball Inclusion of Level- n Elements). *Let x be a point in the interior of the fundamental chamber. Define $B_n := B_K(x, t_n) \subset \mathcal{C}$ to denote the Hilbert ball of radius.*

$$t_n := \inf\{\delta(\omega) : \omega \in \mathcal{D}_{n,n}\}.$$

Then for any $\omega \in W(E_{10})$, if $\omega \cdot x \in B_n$, the s_0 –level of ω satisfies $h_{s_0}(\omega) \leq n$.

This theorem highlights that the s_0 –level filtration is not merely a combinatorial construct, but admits a geometric realization: the s_0 –level of an element $\omega \in W(E_{10})$ provides a coarse bound on its hyperbolic distance from the base chamber in the Tits cone. In this way, the spectral growth hierarchy aligns with a nested system of Hilbert balls, offering a geometric model for the emergence of new spectral values and the expansion of reflection complexity at higher levels.

By a theorem of McMullen [20, Prop. 4.1] (see also Bushell [5]), for a cone–preserving linear transformation A acting on Ω the Hilbert displacement and spectral radius are logarithmically comparable: there exist constants $c_1, c_2 > 0$, depending only on the cone, such that

$$c_1^{-1} \log \rho(A) \leq d_K(x, A \cdot x) \leq c_2 \log \rho(A).$$

Applying this to the elements of $\mathcal{D}_{n,n}$ yields

$$c_1^{-1} \log m_n \lesssim t_n \lesssim T_n \lesssim c_2 \log M_n.$$

Hence, the Hilbert radii (t_n, T_n) grow in lockstep with the logarithmic spectral envelopes

$$(\log m_n, \log M_n).$$

The s_0 –level filtration of $W(E_{10})$ therefore induces a *geometric filtration* of the Tits cone by nested Hilbert balls, in which each level n corresponds to the maximal hyperbolic distance realized by elements of s_0 –length n .

This dual description reveals how the algebraic growth of spectral radii in Λ_n manifests as the hyperbolic expansion of reflection walls $g s_0 g^{-1}$ inside the Tits cone. As $n \rightarrow \infty$, the balls B_n exhaust Ω , providing a geometric visualization of the spectral growth filtration in the hyperbolic model of $W(E_{10})$.

APPENDIX APPENDIX A SPECTRAL RADII IN $W(E_{10})$

This appendix lists primitive Salem numbers that appear as spectral radii in the enlarged spectral sets $\tilde{\Lambda}_2$ and $\tilde{\Lambda}_3$, introduced in Section 5.2. A Salem number $\rho > 1$ is called *primitive* if $\rho^{1/k}$ is not a Salem number for any integer $k > 1$. We exclude all non-primitive powers ρ^k , $k \geq 2$, from the tables.

Each entry in the tables corresponds to the largest real root of a reciprocal minimal polynomial. To conserve space, we list only the first half of the coefficients (a_0, \dots, a_d) , as the remainder are determined by palindromy. Entries are sorted in increasing order of spectral radius. The table for s_0 –level 2 is complete; the table for s_0 –level 3 includes the first 50 primitive Salem numbers.

These spectral values represent the new growth of geometric complexity within the $W(E_{10})$ reflection group, as measured through the spectral radius of elements in $W(A_9)\kappa_{\tilde{T}}W(A_9)$. We refer the reader to Section 5.2 and the spectral growth filtration in Section 4.1 for context and discussion.

k	spectral radius ρ_k	degree	reciprocal coeffs	k	spectral radius ρ_k	degree	reciprocal coeffs
1	1.45799	8	1, 0, -1, -1, 0	20	1.80979	8	1, -1, 0, -2, 0
2	1.50614	6	1, -1, 0, -1	21	1.81161	8	1, -2, 0, 1, -1
3	1.52306	8	1, -1, -1, 0, 1	22	1.83108	6	1, -2, 0, 1
4	1.53293	10	1, -1, -1, 0, 0, 1	23	1.83488	8	1, 0, -1, -2, -3
5	1.54720	8	1, -2, 2, -3, 3	24	1.86406	8	1, -1, -2, 0, 2
6	1.55603	6	1, -1, -1, 1	25	1.87574	10	1, -2, -1, 3, 0, -3
7	1.58235	6	1, 0, -1, -2	26	1.88320	4	1, -2, 1
8	1.60545	8	1, -2, 1, 0, -1	27	1.89911	10	1, -2, 0, 0, 1, -1
9	1.63557	6	1, -2, 2, -3	28	1.91650	8	1, -1, -1, -1, 0
10	1.66105	8	1, -2, 1, -1, 1	29	1.92063	8	1, -3, 3, -2, 1
11	1.68491	8	1, -1, -1, 0, 0	30	1.94686	6	1, -1, -1, -1
12	1.69018	10	1, -1, -2, 1, 1, -1	31	1.97209	10	1, -2, 0, 0, -1, 3
13	1.69351	8	1, -1, 0, -1, -1	32	1.97482	6	1, -2, 1, -2
14	1.72208	4	1, -1, -1	33	1.99400	8	1, -2, 1, -2, 1
15	1.75310	10	1, 0, -1, -1, -2, -3	34	1.99852	10	1, -2, 1, -2, 1, -2
16	1.78164	6	1, -1, -1, 0	35	2.01129	8	1, -3, 3, -3, 3
17	1.79607	8	1, -1, -1, 0, -1	36	2.01601	10	1, -3, 2, 1, -3, 3
18	1.80017	8	1, -3, 4, -5, 5	37	2.04249	6	1, -3, 3, -3
19	1.80502	10	1, -2, 0, 1, -1, 1				

TABLE 4. Primitive Spectral radii in $\tilde{\Lambda}_2$. Each row corresponds to the largest real root of a reciprocal polynomial determined by the listed first half of coefficients.

k	spectral radius ρ_k	degree	reciprocal coeffs	k	spectral radius ρ_k	degree	reciprocal coeffs
1	1.91113	10	1, 0, -2, -2, -1, -1	26	2.17824	10	1, -3, 3, -3, 2, -1
2	1.92679	8	1, 0, -2, -2, -1	27	2.18313	8	1, -1, -1, -2, -2
3	1.94999	10	1, -1, -2, -1, 1, 3	28	2.19565	6	1, -1, -1, -3
4	1.95530	8	1, -2, -1, 3, -1	29	2.20113	6	1, -2, -1, 2, -1
5	1.98779	6	1, -2, -3, -2	30	2.20346	10	1, -2, -1, 1, 0, 1
6	2.02203	8	1, -2, 0, 0, 0	31	2.20647	8	1, -2, -1, 0, 3
7	2.04953	8	1, -1, -1, -1, -2	32	2.21982	10	1, -3, 2, 0, -3, 5
8	2.05354	10	1, -2, -1, 2, 0, -1	33	2.22587	6	1, -3, 2, -1
9	2.05632	10	1, -2, 0, 0, 1, 1	34	2.22747	8	1, -1, -1, -2, -3
10	2.06018	8	1, -3, 2, 1, -3	35	2.22879	10	1, -1, -3, -1, 2, 3
11	2.06973	8	1, -2, 0, 1, -3	36	2.23749	8	1, -2, -1, 1, 0
12	2.08102	4	1, -1, -2, -1	37	2.23890	8	1, 0, -2, -2, -4
13	2.10429	8	1, -1, -1, -1, -3	38	2.24275	8	1, -3, 2, -1, 1
14	2.11854	8	1, 0, -2, -2, -3	39	2.24781	10	1, -1, -2, -1, -1, -1
15	2.12150	8	1, -2, 0, 0, -1	40	2.24885	8	1, -2, 0, -1, 0
16	2.12479	10	1, -1, -3, 0, 2, 1	41	2.25119	8	1, -1, -2, -1, -1
17	2.12992	10	1, -2, 0, 0, -1, 0	42	2.25646	6	1, -2, 0, -1
18	2.13466	8	1, -1, -1, -2, -1	43	2.27019	10	1, -3, 1, 2, -3, 0
19	2.13709	8	1, -2, 0, 1, 1	44	2.27501	10	1, -2, 0, 0, -2, 0
20	2.14511	8	1, -1, -2, -1, 1	45	2.27671	8	1, -3, 2, 0, -2
21	2.14850	10	1, -2, -2, 4, 1, -5	46	2.27965	10	1, -2, 0, 0, 2, 0
22	2.15372	4	1, -3, 3, -3	47	2.28496	10	1, -1, -1, -2, -3, -4
23	2.16021	8	1, -1, -3, 0, 3	48	2.29663	4	1, -2, 0, -2
24	2.16782	10	1, -1, -2, -2, 1, 2	49	2.29949	10	1, -2, -2, 3, 1, -3
25	2.17367	8	1, -2, 0, 1, -1	50	2.30812	10	1, -2, 0, -4, -5, -5

TABLE 5. First 50 primitive Salem spectral radii in $\tilde{\Lambda}_3$. Each row lists two entries side-by-side. The reciprocal coefficients column shows coefficients of $a_0, \dots, a_{d/2}$ where $d = \text{degree}$.

APPENDIX APPENDIX B SAGEMATH IMPLEMENTATION

This appendix provides a SageMath implementation of the recursive construction of the sets T_n described in Section 3.1.2. The code defines the reflections κ_I for triples $I \subset \{1, \dots, 10\}$, computes the transformation data $\text{Trans}(\widehat{I})$, applies the adjacency and level filters, and identifies matrices up to the double–coset action of $W(A_9)$ by canonicalizing under independent row/column permutations (indices 1, …, 10; the e_0 row/column is fixed).

Usage. The initial set T_2 corresponds to the two double cosets in Corollary 3.3. Running `T3 = build_T_next(T2)` constructs T_3 ; iterating builds T_{n+1} from T_n . This procedure is straightforward to implement computationally. A SageMath implementation is provided below.

SageMath code.

```

1 from sage.all import *
2 ZZ = IntegerRing()
3
4 J = diagonal_matrix([1] + [-1]*10)
5
6 def bilinear(x, y):
7     x = vector(ZZ, x)
8     y = vector(ZZ, y)
9     return x.dot_product(J * y)
10
11 def reflection_matrix(v):
12     v = vector(ZZ, v)
13     den = bilinear(v, v)

```

```

14     assert den != 0
15     outer = v.column() * (J * v).row() # 11x1 times 1x11 -> 11x11
16     return identity_matrix(ZZ, 11) - (2/den) * outer
17
18 # --- Triples and reflections kappa_I ---
19 indices = list(range(1, 11)) # {1, ..., 10}
20 ALL_TRIPLES = [frozenset(S) for S in Subsets(indices, 3)]
21
22 def kappa_I_matrix(I):
23     """
24     I is a 3-subset of {1, ..., 10}. Reflection through v = e0 - sum_{i in I} ei.
25     """
26     v = [0]*11
27     v[0] = 1
28     for t in I:
29         v[t] -= 1
30     return reflection_matrix(v)
31
32 def Trans(tuple_of_triples):
33     """
34     Matrix of kappa_{I_1} ... kappa_{I_n} (left-multiplying, column convention).
35     """
36     M = identity_matrix(ZZ, 11)
37     for I in tuple_of_triples:
38         M = kappa_I_matrix(I) * M
39     return M
40
41 # --- Adjacency filter: /I_{\cap I_{\{k+1\}}/ in {0,1} ---
42 def adj_gap1_ok(tuple_of_triples):
43     for A, B in zip(tuple_of_triples, tuple_of_triples[1:]):
44         if len(A & B) not in (0, 1):
45             return False
46     return True
47
48 # --- Canonicalization under W(A9): independent row/col perms on 1..10 (0 fixed)
49 ---
```

50

```

50 def canonicalize_double_coset(M):
51     def sort_columns(N):
52         # keys for cols 1..10: (entry at row 0, then rows 1..10)
53         keys = [(N[0,j], tuple(N[1:11, j]), j) for j in range(1,11)]
54         keys.sort()
55         perm_old = [k[2] for k in keys] # old indices in new order
56         P = zero_matrix(ZZ, 11); P[0,0] = 1
57         for new, old in enumerate(perm_old, start=1):
58             P[old, new] = 1
59         return N * P
60
61     def sort_rows(N):
62         # keys for rows 1..10: (entry at col 0, then cols 1..10)
63         keys = [(N[i,0], tuple(N[i,1:11]), i) for i in range(1,11)]
64         keys.sort()
65         perm_old = [k[2] for k in keys]
66         P = zero_matrix(ZZ, 11); P[0,0] = 1
67         for new, old in enumerate(perm_old, start=1):
68             P[new, old] = 1
69         return P * N
70
71     A = M
72     for _ in range(6): # typically stabilizes in 1--2 passes

```

```

72     A1 = sort_columns(A)
73     A2 = sort_rows(A1)
74     if A2 == A:
75         break
76     A = A2
77 return A
78
79 # --- Base set T2 from Corollary (two ordered pairs) ---
80 T2 = [
81     (frozenset([1,4,5]), frozenset([1,2,3])),
82     (frozenset([4,5,6]), frozenset([1,2,3])),
83 ]
84
85 # --- Precompute canonical forms for level 2 double cosets (id, level-1, two level
86 # -2) ---
86 def precompute_level_le2_canon():
87     forbidden = []
88
89     # level 0: identity
90     M_id = identity_matrix(ZZ, 11)
91     forbidden.append(canonicalize_double_coset(M_id))
92
93     # level 1: any kappa_I; all  $W(A9)$ -conjugate  $\rightarrow$  pick {1,2,3}
94     M_1 = Trans((frozenset([1,2,3]),))
95     forbidden.append(canonicalize_double_coset(M_1))
96
97     # level 2: two classes from Corollary C:small-s0
98     M_2a = Trans((frozenset([1,4,5]), frozenset([1,2,3])))
99     M_2b = Trans((frozenset([4,5,6]), frozenset([1,2,3])))
100    forbidden.append(canonicalize_double_coset(M_2a))
101    forbidden.append(canonicalize_double_coset(M_2b))
102
103    # immutable keys for fast comparison
104    return { tuple(M.list()) for M in forbidden }
105
106 FORBIDDEN_LE2 = precompute_level_le2_canon()
107
108 def is_level3_by_exclusion(tup3):
109     """
110     tup3 = (I, I1, I2).
111     Keep iff its canonicalized matrix is NOT in the precomputed level 2 set.
112     """
113     M = Trans(tup3)
114     Mcanon = canonicalize_double_coset(M)
115     key = tuple(Mcanon.list())
116     return key not in FORBIDDEN_LE2
117
118 def admissible_extensions_front_T3(I1, I2):
119     """
120     Build all I with adjacency  $|I \cap I1|$  in {0,1}, then keep exactly those
121     whose product with (I1, I2) has s0-length 3 by exclusion.
122     """
123     cand = [I for I in ALL_TRIPLES if len(I & I1) in (0,1)]
124     out = []
125     for I in cand:
126         tup3 = (I, I1, I2)
127         if not adj_gap1_ok(tup3):
128             continue
129         if is_level3_by_exclusion(tup3):

```

```

130         out.append(I)
131     return out
132
133 # --- Recursive builder:  $T_{\{n+1\}}$  from  $T_n$  ---
134 def build_T_next(Tn, *, strict_adjacency=True):
135     """
136     Input:  $T_n$  is a list of ordered tuples (each entry is a frozenset of size 3).
137     Output: deduplicated list of ordered tuples of length  $n+1$ ,
138             modulo left/right  $W(A_9)$  via canonicalization of  $Trans$ .
139     """
140     reps = {}
141     for tup in Tn:
142         n = len(tup)
143         I1 = tup[0]
144         # Special  $n=2$  step: use the level 2 exclusion to decide true level 3
145         if n == 2:
146             cand = admissible_extensions_front_T3(I1, tup[1])
147         else:
148             cand = ALL_TRIPLES if not strict_adjacency else \
149                   [I for I in ALL_TRIPLES if len(I & I1) in (0,1)]
150         for I in cand:
151             new_tup = (I,) + tup
152             if strict_adjacency and not adj_gap1_ok(new_tup):
153                 continue
154             M = Trans(new_tup)
155             Mcanon = canonicalize_double_coset(M)
156             key = tuple(Mcanon.list())
157             if key not in reps:
158                 reps[key] = new_tup
159     return list(reps.values())
160
161 # --- Example: build  $T_3$  from  $T_2$  ---
162 T3 = build_T_next(T2)
163 print("T3 size:", len(T3))
164 for t in T3:
165     print(t)

```

REFERENCES

- [1] Eric Bedford and Kyounghee Kim. Dynamics of rational surface automorphisms: linear fractional recurrences. *J. Geom. Anal.*, 19(3):553–583, 2009.
- [2] Sara C. Billey, Matjaž Konvalinka, T. Kyle Petersen, William Slofstra, and Bridget E. Tenner. Parabolic double cosets in Coxeter groups. *Electron. J. Combin.*, 25(1):Paper No. 1.23, 66, 2018.
- [3] Anders Björner and Francesco Brenti. *Combinatorics of Coxeter groups*, volume 231 of *Graduate Texts in Mathematics*. Springer, New York, 2005.
- [4] Jérémie Blanc and Serge Cantat. Dynamical degrees of birational transformations of projective surfaces. *J. Amer. Math. Soc.*, 29(2):415–471, 2016.
- [5] P. J. Bushell. Hilbert’s metric and positive contraction mappings in a Banach space. *Arch. Rational Mech. Anal.*, 52:330–338, 1973.
- [6] Vinay V. Deodhar. On some geometric aspects of Bruhat orderings. II. The parabolic analogue of Kazhdan-Lusztig polynomials. *Journal of Algebra*, 111(2):483–506, 1987.
- [7] Jeffrey Diller. Cremona transformations, surface automorphisms, and plain cubics. *Michigan Math. J. The Michigan Mathematical Journal*, 60(2):409–440, 2011.
- [8] Jeffrey Diller and Charles Favre. Dynamics of bimeromorphic maps of surfaces. *Amer. J. Math.*, 123(6):1135–1169, 2001.
- [9] Igor Dolgachev. Reflection groups in algebraic geometry. *Bulletin of the American Mathematical Society*, 45(1):1–60, 2008.

- [10] Brian Drake and Evan Peters. An upper bound for reflection length in Coxeter groups. *J. Algebraic Combin.*, 54(2):599–606, 2021.
- [11] Kamil Duszenko. Reflection length in non-affine Coxeter groups. *Bull. Lond. Math. Soc.*, 44(3):571–577, 2012.
- [12] Matthew Dyer. On the bruhat graph of a coxeter system. *Compositio Mathematica*, 78(2):185–191, 1991.
- [13] Meinolf Geck and Götz Pfeiffer. *Characters of finite Coxeter groups and Iwahori-Hecke algebras*, volume 21 of *London Mathematical Society Monographs. New Series*. The Clarendon Press, Oxford University Press, New York, 2000.
- [14] James E. Humphreys. *Reflection groups and Coxeter groups*, volume 29 of *Cambridge Studies in Advanced Mathematics*. Cambridge University Press, Cambridge, 1990.
- [15] David Kazhdan and George Lusztig. Representations of Coxeter groups and Hecke algebras. *Invent. Math.*, 53(2):165–184, 1979.
- [16] Kyounghie Kim. Salem/pisot numbers in the weyl spectrum. *preprint*, <https://arxiv.org/pdf/2312.17729.pdf>.
- [17] Kyounghie Kim. The dynamical degrees of rational surface automorphisms. *Conform. Geom. Dyn.*, 28:62–87, 2024.
- [18] Marco Lotz. Reflection length at infinity in hyperbolic reflection groups. *J. Group Theory*, 28(1):67–89, 2025.
- [19] Jon McCammond and T. Kyle Petersen. Bounding reflection length in an affine Coxeter group. *J. Algebraic Combin.*, 34(4):711–719, 2011.
- [20] Curtis T. McMullen. Coxeter groups, Salem numbers and the Hilbert metric. *Publ. Math. Inst. Hautes Études Sci.*, (95):151–183, 2002.
- [21] Curtis T McMullen. Dynamics on blowups of the projective plane. *Publications Mathématiques de l’Institut des Hautes Études Scientifiques*, (105):49–90, 2007.
- [22] Masayoshi Nagata. On rational surfaces. I. Irreducible curves of arithmetic genus 0 or 1. *Mem. Coll. Sci. Univ. Kyoto Ser. A Math.*, 32:351–370, 1960.
- [23] Masayoshi Nagata. On rational surfaces. II. *Mem. Coll. Sci. Univ. Kyoto Ser. A Math.*, 33:271–293, 1960/1961.
- [24] Wolfgang Soergel. Kategorie \mathcal{O} , perverse Garben und Moduln über den Koinvarianten zur Weylgruppe. *J. Amer. Math. Soc.*, 3(2):421–445, 1990.
- [25] Takato Uehara. Rational surface automorphisms with positive entropy. *Ann. Inst. Fourier (Grenoble)*, 66(1):377–432, 2016.
- [26] È. B. Vinberg. Discrete linear groups that are generated by reflections. *Izv. Akad. Nauk SSSR Ser. Mat.*, 35:1072–1112, 1971.

DEPARTMENT OF MATHEMATICS, FLORIDA STATE UNIVERSITY, TALLAHASSEE, FL 32308
Email address: kkim6@fsu.edu